Available online at www.sciencedirect.com

SCIENCE DIRECT®

Geochimica et Cosmochimica Acta 70 (2006) 1188–1214

Geochimica

www.elsevier.com/locate/gca

A catalytic delamination-driven model for coupled genesis of Archaean crust and sub-continental lithospheric mantle

Jean H. Bédard

Geological Survey of Canada, GSC-Québec, 490 de la Couronne, Québec, PQ, Canada G1K 1A9

Received 12 May 2005; accepted in revised form 7 November 2005

Abstract

There is no consensus on the processes responsible for near-coeval formation of Archaean continental crust (dominantly tonalite–trondhjemite–granodiorite: TTG), greenstone belts dominated by komatiitic to tholeiitic lavas (KT), and sub-continental lithospheric mantle (SCLM). The Douglas Harbour domain (2.7–2.9 Ga) of the Minto Block, northeastern Superior Province, has two TTG suites, the western and eastern Faribault–Thury (WFT and EFT), with embedded KT greenstones. Tonalites of both suites have high light/heavy rare-earth element ratios (L/HREE), high large ion lithophile element (U–Th–Rb–Cs–La: LILE) contents, positive Sr–Pb anomalies, and negative Nb–Ta–Ti anomalies. Such typical Archaean TTG signatures are commonly explained by melting of subducted oceanic crust, but could also originate by melting the base of thick basaltic plateaux formed above mantle upwellings (plumes), leaving behind restites containing pyroxene, garnet, and rutile. Field relationships (in situ segregation veins), phase equilibria (hornblende stabilized at lower crustal pressure), petrography (corroded epidote and muscovite phenocrysts, rare plagioclase phenocrysts), and trace element models, all imply that FT tonalite to trondhjemite evolution reflects hornblende-dominated fractional crystallization, not partial melting of subducted crust. The geochemistry of parental FT tonalites can be modeled by 15–30% melting of FT tholeiitic metabasalts, with residues of eclogite, garnet-websterite, or hornblende-garnet websterite. A minor residual Ti-phase such as rutile is also needed to generate negative Ti–Nb–Ta troughs in the TTGs. However, large volumes of eclogitic restites complementary to TTG are not observed either at the base of Archaean crustal sections, or in the SCLM. Additional problems with slab-melting models include: (a) the rarity of lithologies and associations characteristic of active margins (ophiolites, andesites, blueschists, accretionary mélanges, molasse, flysch, high-pressure belts, and thrust-and-fold belts); (b) the need to deliver plume-derived KT melt through the slab; and (c) extracting enough TTG melt from a subducting slab in the time available (200–300 my). In the plateau-melting model, heat for crustal anatexis is supplied by ongoing KT magma derived from mantle upwellings. However, SCLM rocks differ from predicted 1-stage mantle melting residua; and the voluminous residual eclogites complementary to TTG generation somehow need to be removed. These two problems might solve one another if the dense crustal restites disaggregated and mixed into the underlying depleted mantle. Mantle melting slows upon exhaustion of Ca–Al-rich phases, with large temperature increases needed to extract more melt from harzburgite residua. Physical addition of delaminated crustal restites would refertilize the refractory mantle, allowing extraction of additional melt increments, and might explain the ultra-depleted and orthopyroxene-rich nature of the SCLM. A hybrid source composed of 10% eclogitic restite of EFT tonalite generation, mixed with harzburgitic residues from 25% melting of primitive mantle, yields model melts with trace element signatures resembling typical Munro komatiites. Variations in the mineralogy and geochemistry of the delaminated component might account for the diversity of komatiite types. Degassing of hornblende-rich delaminated restites would transfer LILE to surrounding depleted mantle and could generate boninites. Fusion of undepleted metabasalt sandwiched among denser restites could generate sanukitoids. Mantle melt pulses generated by catastrophic delamination events would underplate nascent TTG crust and trigger renewed crustal melting, followed by delamination of newly formed eclogitic restites, triggering additional mantle melting, and so on. I posit that delamination of crustal restites catalyzed multi-stage melting of the SCLM and maturation of the Archaean continental crust. Thus, Archaean crust and SCLM are genetically inter-linked, and both form above major mantle upwellings.

E-mail address: jean.bedard@rncan.gc.ca

0016-7037/$ - see front matter Crown Copyright © 2005 Published by Elsevier Inc. All rights reserved.
doi:10.1016/j.gca.2005.11.008

1. Introduction

There is no consensus about the mechanisms that created Archaean crust and sub-continental lithospheric mantle (SCLM). Existing age data imply that the SCLM formed synchronously or immediately after (100–300 Ma) the crust (Richardson et al., 1984; Bell and Blenkinsop, 1987; Huang et al., 1995; Pearson et al., 1995; Pearson, 1999; Moser et al., 2001; Schmidberger et al., 2002; Davis et al., 2003). The buoyant nature, high viscosity, and high brittle yield stress of Fe-depleted, refractory, Archaean SCLM keep it from being recycled into the convecting asthenosphere, and also protects the cratonic crust (Davies, 1979; Jordan, 1988; Abbott et al., 1997; De Smet et al., 2000; Moser et al., 2001; Poudjom Djomani et al., 2001; Lenardic et al., 2003). However, the ultra-depleted SCLM differs from 1-stage melting residua of primitive mantle in having olivine Fo-contents that are too high (>Fo92) for a given modal olivine content, with local excesses in SiO_2 and modal orthopyroxene/olivine at high Mg# (MgO/MgO + FeO) (Boyd, 1998; Kelemen et al., 1998; MacKenzie and Canil, 1999; Zheng et al., 2001; Arndt et al., 2002; Griffin et al., 2003; Herzberg, 1999, 2004).

Archaean crust is dominated by granite–greenstone terranes organized into dome-and-keel structures that do not resemble the linear orogenic belts that typify Proterozoic and Phanerozoic orogens (Anhaeusser et al., 1969; Goodwin, 1981, 1996; Windley, 1984; Kröner, 1985; Ayres and Thurston, 1985; Bickle et al., 1995; Choukroune et al., 1995; Hamilton, 1998; Bleeker, 2002). Proposed genetic models for granite–greenstone terranes run the gamut from early vertical tectonic scenarios involving ensialic processes (e.g., Macgregor, 1951; Baragar and McGlynn, 1976; Goodwin, 1981); to uniformitarian plate-tectonic models involving arcs (Glikson, 1972; Tarney et al., 1976; Dimroth et al., 1982; Windley, 1984); to a presently popular model involving marginal oceanic terrane accretion and mixed arc-plume magmatism (e.g., Drury et al., 1984; Davis et al., 1988; Card, 1990; Williams, 1990; Desrochers et al., 1993; Kimura et al., 1993; de Wit, 1998; Kusky, 1998; Kusky and Polat, 1999; Lowe, 1999; Daigneault et al., 2002; Chown et al., 2002; Dirks et al., 2002; Percival et al., 2004). Recently, vertical magmatic-tectonic scenarios for craton cores involving partial convective overturn have regained favour (Davidson, 1980; Hickman, 1983, 1984, 2004; Bouhallier et al., 1995; Chardon et al., 1996, 1998, 2002; Collins et al., 1998; Bleeker, 2002; Rey et al., 2003; Bédard et al., 2003; Van Kranendonk et al., 2004; Ketchum et al., 2004); and increased attention is being focused on proposals for progressive maturation of Iceland-type crust above major mantle upwellings (Lambert, 1981; Maaløe, 1982; Kröner, 1985; this paper).

Interpreting the origin of individual Archaean cratons requires detailed stratigraphic and structural constraints (e.g., Van Kranendonk et al., 2002, 2004; Bleeker, 2002; Hickman, 2004; Percival et al., 2004; Ketchum et al., 2004), but also depends heavily on the attribution of tectonic environments to the constituent magmatic rocks. Unfortunately, palaeo-tectonic geochemical and petrological fingerprinting is not unambiguous, even in the Phanerozoic (e.g., Wang and Glover, 1992). For example, Archaean felsic plutons and gneisses are commonly interpreted to have formed in oceanic or continental arc environments, with an origin as either: (a) the fusion products of subducted oceanic crust (e.g., Weaver and Tarney, 1981; Condie, 1981; Martin, 1999; Foley et al., 2002); (b) the fractionation products of subduction-related mantle melts (Feng and Kerrich, 1992; Kamber et al., 2002; Kleinhanns et al., 2003); or (c) the result of intra- and lower-crustal anatexis of oceanic arcs or thickened crust (Smithies, 2000; Whalen et al., 2002, 2004a). The dominant tholeiitic and komatiitic lavas of the associated greenstone belts, on the other hand, are generally interpreted to have formed above mantle plumes (e.g., Campbell et al., 1989; Tomlinson et al., 1999; Kerrich and Xie, 2002; Wyman and Kerrich, 2002; Wyman et al., 2002; Sproule et al., 2002; Arndt, 2003; Herzberg, 2004). Since the komatiites and tholeiites are commonly interbedded with felsic tuffs and lavas (e.g., Hamilton, 1998; Tomlinson et al., 2004) some of which can be correlated to the ages and chemistry of the adjoining felsic plutons (e.g., Hill et al., 1989; Van Kranendonk et al., 2004); and since the felsic volcanic and plutonic rocks are generally inferred to have arc affinities (e.g., Barrie et al., 1993; Lesher et al., 1986), then uniformitarian interpretations require extremely complex geodynamic scenarios involving multiple subduction zones, slab windows and intermittent plumes (e.g., Wyman et al., 2002). The sum of these complexities has led to the extreme conclusion that there is no genetic link between the Archaean continental crust and the near-coeval SCLM that underlies it (Arndt et al., 2002). In this paper, I will propose a hypothesis to explain this problematic association, the diachronous origin of cratons (3.8–2.7 Ga), and the apparently paradoxical co-emplacement of arc and plume-related magmatic suites. Archaean rocks (2.9–2.7 Ga.) of the Minto Block, north-eastern Superior Province (Fig. 1) will be used to illustrate some of these relationships, and as the basis for geochemical tests of the hypotheses proposed.

2. Are archaean tonalite–trondhjemite–granodiorite suites subduction-related?

2.1. Archaean crust

Archaean crust is dominated by the tonalite–trondhjemite–granodiorite suite (TTG: Barker and Arth, 1976; Jahn et al., 1981; Condie, 1981; Martin, 1987; Luais and Hawkesworth, 1994). The 'calc-alkaline' nature of Archaean TTGs has led to the widely held hypothesis that they represent the eroded root zones of Archaean Andean-Type margins (Weaver and Tarney, 1980; Condie, 1980; Stern et al., 1994; Martin, 1999). However, most Archaean TTG suites are not calc-alkaline, but belong to a distinctly more sodic tonalite–trondhjemite (TT) differentiation trend

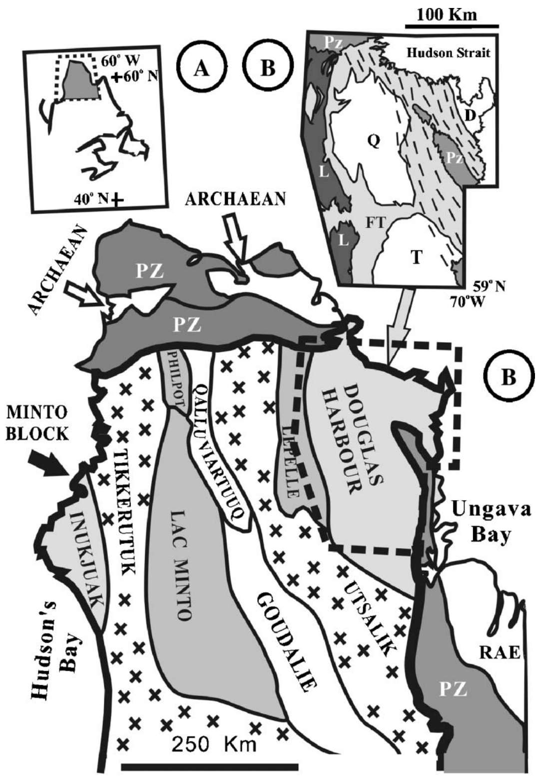

Fig. 1. Geological sketch map of the Minto Block, NE Superior Province, Canada, adapted from Percival and Skulski (2000), showing the different crustal domains. Pz, Proterozoic rocks; Rae, Archaean rocks of the Rae Province. Inset (A) shows the location, while inset (B) shows a detail of the Douglas Harbour Domain of the NE Minto (Madore et al., 1999, 2001; Madore and Larbi, 2000; Bédard et al., 2003), showing the distribution of Western and Eastern Faribault–Thury Complex rocks (FT), dominated by 2.9–2.86 Ga and 2.83–2.72 Ga tonalites and trondhjemites (respectively). The Troie and Quimussinguat complexes (T and Q) are dominated by 2.74–2.73 Ga enderbites (pyroxene tonalites and trondhjemites). *L*, lepelle complex granodiorites and tonalites. *D*, Diana complex tonalites, inferred to belong to the Rae Province.

(Arth et al., 1978; Martin, 1987; Luais and Hawkesworth, 1994); with locally prominent development of high-temperature pyroxene–tonalites or enderbites (Ridley, 1992; Percival and Mortensen, 2002; Bédard et al., 2003). Archaean granitoids display secular K-enrichment, with the younger plutons in a craton gradually becoming more calc-alkaline (e.g., Davis and Edwards, 1986; Taylor and McLennan, 1986; Stern and Hanson, 1991; Collins, 1993; Stevenson et al., 1999; Madore et al., 1999; Moyen et al., 2001; Whalen et al., 2004b; Martin et al., 2005). Phase equilibrium constraints and trace element models indicate that TT magmas were derived by anatexis of metabasalt, leaving behind eclogite (garnet–clinopyroxenite), amphibolite, or garnet amphibolite residues (Arth and Hanson, 1972, 1975; Beard and Lofgren, 1991; Rapp et al., 1991; Rushmer, 1991; Foley et al., 2002; Rapp et al., 2003; Moyen and Stevens, 2005).

2.2. Adakites

The overall high Sr/Y, La/Yb, and lack of Eu anomalies of most Archaean TTs has been taken to signify that they are similar to high-SiO_2 adakites (Drummond and Defant, 1990; Martin, 1999; Martin and Moyen, 2002; Martin et al., 2005). High-SiO_2 adakites have $SiO_2 > 60\%$, $MgO < 4\%$, $TiO_2 < 0.9\%$, high Sr (<1000 ppm), high contents of LREE (light rare earth elements) and LILE (large ion lithophile elements), and low Y (<20 ppm) and HREE (heavy rare earth elements). High-SiO_2 adakites are thought to have formed by multistage devolatilization and melting of unusually young (hot) oceanic crust as it subducts (Drummond and Defant, 1990; Drummond et al., 1996; Kepezhinskas et al., 1997; Rollinson and Tarney, 2005; Martin et al., 2005). The high Mg#, Cr, and Ni of some high-SiO_2 adakites is attributed to reaction with the mantle wedge (Kay, 1978; Carroll and Wyllie, 1989; Calmus et al., 2003; Martin et al., 2005). Adakites are rare in the Phanerozoic, since oceanic crust will only melt if it is unusually young and hot (Fig. 2; Defant and Kepezhinskas, 2001). The higher temperatures inferred for the Archaean mantle has led to the proposal that slab melting was more common then (e.g., Martin, 1993).

2.3. Can Archaean slabs melt?

Martin (1986, 1993) proposed a hot Archaean geotherm consistent with abundant melting of the subducted slab (Fig. 2). However, modeled pressure–temperature paths of the upper surface of subducting crust only enter regions with melt fractions >5% if the crust is very young and hot, and if convergence rates are extremely slow (<2 cm/year: Fig. 2; Peacock et al., 1994; Kincaid and Sacks, 1997; van Keken et al., 2002; Kelemen et al., 2004b). While these calculations are consistent with the concept of limited slab melting under the most favourable conditions imaginable, a number of caveats must be remembered. (1) Not all Archaean oceanic crust could have been so young, and much of it must have been too cold to melt, yielding normal 'arc' magmas instead. (2) Calculations and some paleomagnetic data suggest that Archaean plates moved faster than Phanerozoic plates (e.g., Bickle, 1978, 1986; Strik et al., 2003); which would not be conducive to slab melting during subduction. (3) It has also been suggested that hot slabs would dehydrate quickly, losing the water needed to flux slab melting at greater depths (Harry and Green, 1999). (4) Pressure–temperature paths that attain melt fractions >5% only pertain to the top of the subducting slab. Thermal diffusion into subducting slabs is extremely slow, otherwise they would not retain their rheological, seismic or mechanical identity long enough to drive subduction (Carlson et al., 1983). Thus, subducted lower oceanic crust would not heat up to the same extent as the upper crust (Fig. 2; van Keken et al., 2002), and so should not have melted significantly. (5) None of the computed pressure–temperature paths reach temperatures appropriate for genesis of the voluminous enderbitic suite (⩾1050 °C: Bédard, 2003).

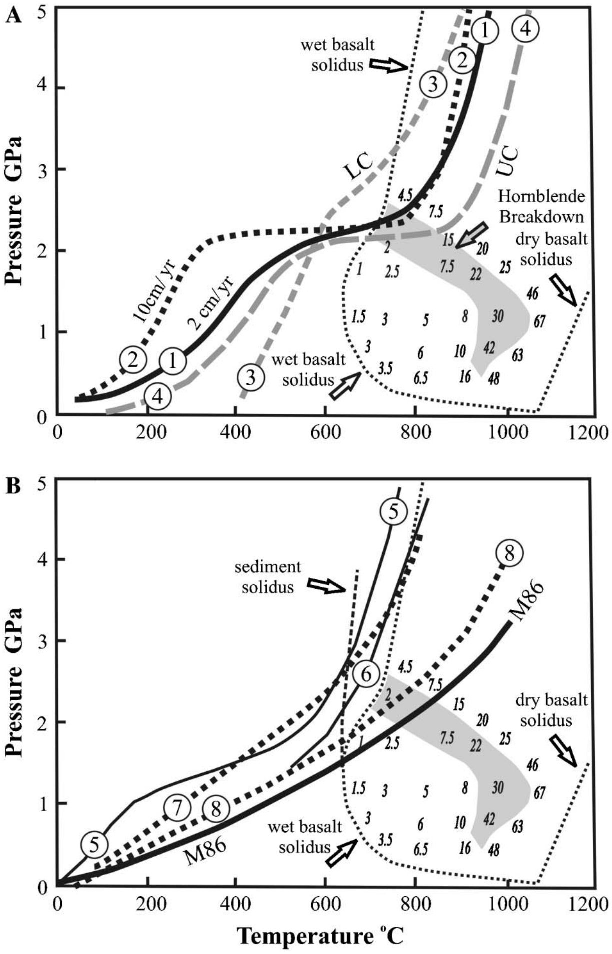

Fig. 2. Comparison of a basaltic phase diagram with model pressure–temperature (PT) paths calculated for the upper surface of the subducting oceanic crust. Only the models most favourable to slab melting are shown. Models for older or faster slabs rarely intersect the basaltic solidus. Dotted curves show the wet and dry basaltic solidus, the grey field marks hornblende breakdown reactions, with the small italic numbers in the supra-solidus domain indicating the % melt present at the PT conditions shown (Peacock et al., 1994). The solidus and melt proportions are appropriate for an amphibolite with 50/50 hornblende/plagioclase, with 0.3 wt% H_2O added (Peacock et al., 1994). The phase relations shown are not significantly different from an Archaean tholeiite phase diagram (Rapp and Watson, 1995). The sediment solidus (dashed line) is from Nichols et al. (1994). (A) The solid (1) and dotted (2) black curves are the PT trajectories appropriate for the upper part of the subducting oceanic crust from van Keken et al. (2002) for convergence rates of 2 and 10 cm/year (respectively), a slab age of 20 Ma, and a subduction angle of 30°. Grey dashed curves LC (3) and UC (4) are for the lower and upper crust (respectively) of a 10 Ma old slab converging at 0.45 cm/year (van Keken et al., 2002). (B) Solid lines (5 and 6) are model PT trajectories for the upper part of a 50 Ma slab (Kelemen et al., 2004b), and a convergence rate of 6 cm/year. The curve labelled (6) includes the effect of shear heating. The heavy dashed lines (7 and 8) are model PT trajectories (Kincaid and Sacks, 1997) for the upper part of a slab dipping 45°, moving at 1.3 cm/year, for thermal boundary layer thicknesses of 70 and 45 km, respectively. The heavy black line marked 'M86' is the putative Archaean geotherm from Martin (1986).

2.4. Shallow Archaean subduction?

Most estimates suggest that Archaean oceanic crust was thicker than Phanerozoic oceanic crust (e.g., Windley and Davies, 1978; Sleep and Windley, 1982; Bickle, 1986; Davies, 1992; Vlaar et al., 1994). Such thick crust would imply shallow subduction angles (e.g., Hoffman and Ranalli, 1988; Cloos, 1993; Abbott et al., 1994), and it has been suggested that failed subduction of thick, buoyant oceanic crust would lead to subcretion/obduction, and represent a major crustal growth process (e.g., Helmstaedt and Schulze, 1986; Hoffman and Ranalli, 1988; Davies, 1992; Smithies et al., 2003). Subduction of a hot slab, the axiom of the adakite model, also favours a shallow subduction angle, since hot slabs are more buoyant (e.g., Kincaid and Sacks, 1997). On the other hand, Van Hunen et al. (2004) suggest that flat subduction may not be required if the mantle potential temperature is $\geqslant 1375$ °C. More research is needed to confirm the plausibility of Archaean subduction, flat or otherwise (cf. Stern, 2005).

If hotter and thicker Archaean oceanic crust implies shallow subduction, then the downgoing slab must underthrust the overriding plate and there would be little or no overlying mantle wedge. Since the primary source of heat for anatexis of the subducting slab is convection of the overlying mantle wedge induced by movement of the slab (e.g., Kincaid and Sacks, 1997), then shallow subduction should inhibit the transfer of heat into the subducting crust (e.g., Dumitru et al., 1991; Cahill and Isacks, 1992; Gutscher and Peacock, 2003), and so preclude its anatexis.

2.5. Melt productivity deficits

The requirement for a slow rate of convergence creates a mass-balance problem with regard to generation of thick Archaean TTG crust from subducting metabasalt. The Minto block of the north-eastern Superior Province is about 500 km wide (Fig. 1), and most of its rocks were generated between 2.9 and 2.7 Ga. It has an overall N-NW structural grain, which has been interpreted (e.g., Percival and Skulski, 2000) to record multiple, E-W directed, subduction/collision events. In the context of the adakite model, a 500 km wide, 40 km thick continental crust implies that 20,000 km^3 of magma needs to be generated for each km of strike-length of an Archaean subduction zone. If we assume a generous 300 Ma time-window, that all of the melt is derived by slab melting, and that none is trapped in the mantle; then this implies a minimum melt production of 67 km^3/Ma/km of subduction zone. This minimum value considerably exceeds typical melt fluxes from Phanerozoic subduction zones (e.g., 20 km^3/Ma: Patino et al., 2000; 4 km^3/Ma Macdonald et al., 2000), but is similar to estimates from Iceland (92 km^3/Ma: Jakobsson, 1972). Furthermore, combining a slow 1.2 cm/year convergence rate (the average Archaean convergence rate computed by Hargraves, 1986) with a 10-km thick oceanic crust that melts 10%, yields only 3600 km^3 of magma per km of subduction zone, nearly an order of magnitude smaller than the amount required (20,000 km^3). There are two possible ways to circumvent this problem. (1) There may have been 6 subduction zones simultaneously active for 300 Ma in the

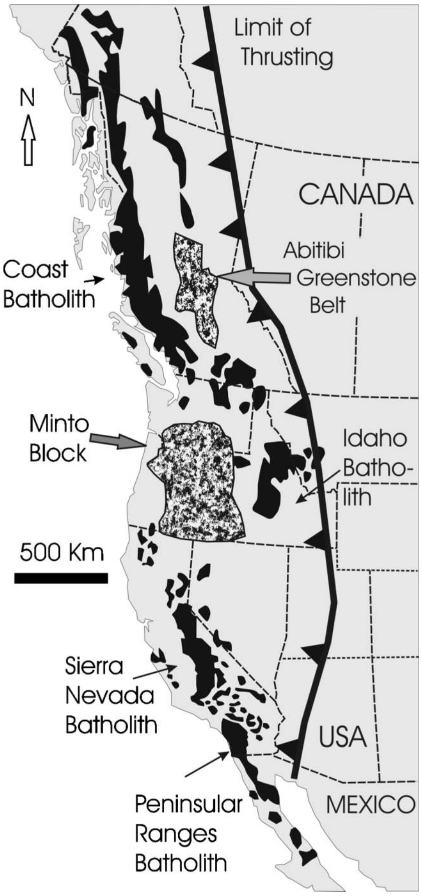

Fig. 3. A sketch map of the North American Cordillera (adapted from Winter, 2001), showing the distribution of major felsic plutons, and the limit of Mesozoic thrusting. The Minto Block and Abitibi greenstone belt are overlain to show their comparatively small size.

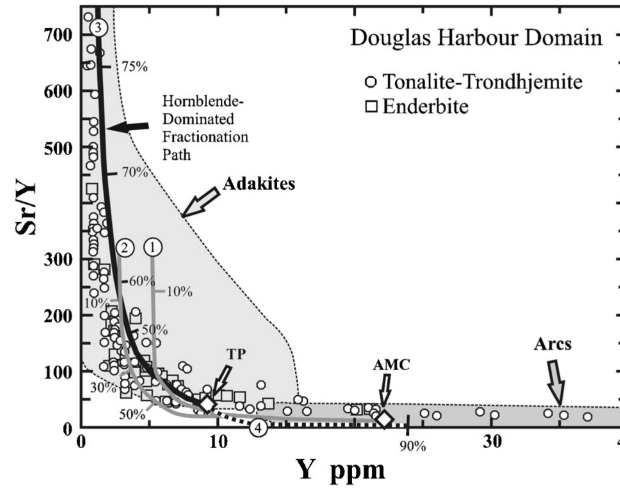

Fig. 4. Sr/Y vs. Y diagram showing the distribution of tonalites, trondhjemites and enderbites (pyroxene–tonalites) from the Douglas Harbour Domain (Minto Block, NE Superior Province). Thick grey curves show the distribution of batch melts derived from an Archaean Mafic Composite (AMC) source (Drummond and Defant, 1990) in equilibrium with eclogite (1) and garnet amphibolite (10% gt, 2) restite assemblages. The Adakite and Arc fields are from Castillo et al. (1999). The heavy black curve (3) is a hornblende-dominated fractional crystallization path from a tonalitic parental melt (TP). The dotted black curve (4) shows a fractionation path for up to 90% dioritic fractionation (50:50 hornblende + plagioclase). Both fractionation models (3 and 4) were calculated using the constant D values shown in Table 1.

Minto case. While possible, this seems excessive, given the comparative scale of Phanerozoic active margins (Fig. 3). (2) Convergence rates may have been 6 times faster or more. Thermal and continental freeboard arguments (e.g., Bickle, 1986; Howell, 1989), and some recent palaeomagnetic data (Strik et al., 2003), also suggest rapid Archaean plate migration rates, up to 100 cm/year; although most paleomagnetic studies imply rates comparable to modern environments (e.g., Kröner, 1991; Piper, 2003). In any case, rapid subduction cannot solve the magmatic deficit, because rapid subduction rates imply that the slab will not heat up enough to melt (Fig. 2).

2.6. Fractional crystallization as an origin for high Sr/Y magmas

The geochemical similarity between Archaean TTGs and adakites has been considered a ‘smoking gun’ indicating an arc origin for TTGs, although Smithies (2000) and Condie (2005) consider them as distinct magma types. For example, the high Sr/Y ratio of many Archaean TTGs (Fig. 4) is commonly attributed to anatexis of subducting oceanic crust with plagioclase-free residues (e.g., Drummond and Defant, 1990). However, to explain the very high Sr/Y (and other geochemical signatures) by partial melting requires that very small fractions of melt (<5%) generated in a subducting slab must be able to wend their way through c. 100 km of a convecting mantle wedge, and then through >30 km of a partially molten crust, without losing their geochemical identity. This seems implausible. An additional constraint is that the TTGs with the highest Sr/Y are the evolved trondhjemitic facies with $SiO_2 >$ 70–72% (Fig. 5: cf. Tarney et al., 1979), which suggests to me that Sr/Y enrichment is the result of fractional crystallization, an hypothesis that is explored next using rocks of the Minto Block as an example.

Minto TT suite rocks grade continuously from hornblende-biotite tonalites to biotite ± muscovite trondhjemites. The common presence of partly resorbed igneous epidote and muscovite implies that these magmas ascended rapidly as crystal slurries (Brandon et al., 1996; Bédard, 2003). Trondhjemite-filled melt segregation structures in tonalites (Bédard et al., 2003) indicate a syn- to post-emplacement melt segregation origin, and are clearly inconsistent with independent derivation of trondhjemite from a subducting slab. There is progressive development of positive Sr–Eu anomalies and heavy rare-earth element (and Y) depletion (Figs. 5 and 7) as rocks grade from tonalite to trondhjemite. Fractionation models involving abundant plagioclase cannot generate such trends, but hornblende-dominated fractionation models yield appropriate trace element signatures (Figs. 5 and 7). The tonalites with Y > 15 ppm shown on Fig. 4 may represent either low-pressure, plagioclase-bearing fractionation paths, or cumulates associated with segregation of trondhjemitic residual melts from the ascending tonalitic, high-pressure crystal slurry. Comparison with phase equilibrium data from tonalitic bulk compositions (Schmidt and Thompson, 1996; Bédard, 2003), the notable lack of plagioclase phenocrysts and occasional presence of hornblende phenocrysts in Minto tonalites (Bédard et al., 2003), and results of trace element modeling (Figs. 4 and 7), are all consistent with the theory that TT magmatic evolution records hornblende-dominated fractional crystallization of a tonalitic parental melt in the lower-middle crust (Arth et al., 1978; Tarney et al., 1979; Sutcliffe et al., 1990; Castillo et al., 1999).

2.7. Importance of residual titanate minerals

In Phanerozoic magmas, negative Nb–Ta–Ti anomalies are widely considered an arc signature (Pearce, 1982). However, rutile, ilmenite or titanite are present for a wide range of conditions in felsic melts derived from anatexis of metabasalt (Green and Pearson, 1986; Ryerson and Watson, 1987; Patiño-Douce and Johnston, 1991; Rapp et al., 1991; Klemme et al., 2002), and have very high *D*s for these elements (Table 1; Horng and Hess, 2000; Foley et al., 2000; Klemme et al., 2002; Tiepolo et al., 2002; Jang and Naslund, 2003; Prowatke and Klemme, 2005). Since residual titanates could equally well form at the pressure and temperature conditions characteristic of melting at the base of oceanic plateaux, then negative Nb–Ta–Ti anomalies in TTGs are not necessarily diagnostic of an arc environment.

2.8. Origin of TTG by fractionation of andesite?

It has also been proposed that Archaean TTGs are fractionation products of subduction-related, hydrous, basaltic

Table 1
Partition coefficients used to model fractionation of tonalites and anatexis of metabasites

D	Cpx	Opx	Plag	Amp	Biot	Garnet	Magn	Ilmen	Titan	Zircon	Epidote	Allanite	Apatite	Rutile
Cs	0.0026	0.047	0.087	0.166	0.63	0.0001	0.001	0.025	0.3	4.4	0.0045	0.0380	0.05	0.01
Rb	0.0100	0.047	0.068	0.055	2.25	0.0007	0.001	0.025	0.5	4.0	0.0045	0.0765	0.1	0.0076
K	0.0039	0.047	0.252	0.333	3.0	0.0013	0.001	0.034	0.7	4.0	0.0045	0.05	0.2	0.005
Ba	0.006	0.047	1.016	0.046	6.0	0.0004	0.001	0.018	1.5	4.0	0.408	11.21	0.45	0.0043
Th	0.104	0.130	0.095	0.055	0.010	0.0075	0.02	0.09	0.16	62	156	2418	23	0.2
U	0.032	0.089	0.091	0.050	0.100	0.024	0.02	0.09	0.14	298	1.29	20	25	0.2
Nb	0.007	0.010	0.239	0.274	0.085	0.040	0.04	3.0	2.2	50	0.226	3.5	0.05	42.8
Ta	0.028	0.126	0.053	0.477	0.107	0.080	0.04	2.7	6.55	50	0.226	3.5	0.05	68.0
La	0.028	0.0003	0.358	0.319	0.020	0.028	0.015	0.015	4.73	26.6	2.05	1005	12	0.0057
Ce	0.059	0.0007	0.339	0.560	0.030	0.080	0.016	0.012	7.57	23.5	2.44	725	15	0.0065
Pr	0.116	0.0014	0.316	0.898	0.008	0.150	0.018	0.011	9.0	20.0	2.86	489	17	0.0073
Pb	0.022	0.047	0.770	0.175	0.10	0.032	0.022	0.0078	0.04	0.001	0.50	0.53	0.1	0.0154
Sr	0.032	0.047	6.65	0.389	0.10	0.019	0.022	0.0022	2.68	20	2.0	10.3	1.4	0.036
P	0.162	0.050	0.079	0.225	0.005	0.184	0.024	0.002	0.057	20	0.18	1.0	410	0.03
Nd	0.115	0.0028	0.289	1.32	0.030	0.222	0.026	0.010	12.4	21.7	3.34	308	19	0.0082
Sm	0.259	0.0085	0.237	2.09	0.040	1.43	0.024	0.009	14.0	17.7	4.22	116	20	0.0954
Zr	0.125	0.031	0.078	0.417	0.023	0.537	0.12	2.3	1.92	130	0.10	0.13	16	3.7
Hf	0.208	0.246	0.069	0.781	0.023	0.431	0.97	2.4	2.43	450	10.0	18.9	16	4.97
Ti	0.473	0.500	0.078	4.03	3.5	2.63	5.0	12.5	67.0	10.0	0.375	1.66	14	45
Eu	0.341	0.680	2.17	1.79	0.031	1.54	0.025	0.010	13.8	12.1	3.78	4.34	13	0.00037
Gd	0.422	0.020	0.192	2.53	0.04	4.84	0.018	0.011	11.9	15.0	4.67	42.4	20	0.0106
Tb	0.502	0.030	0.170	2.60	0.05	7.80	0.019	0.018	10.0	37.3	4.67	24.3	19	0.0111
Dy	0.570	0.043	0.150	2.55	0.06	11.5	0.018	0.020	8.27	60	4.50	13.4	18	0.0116
Y	0.603	0.054	0.138	2.47	0.07	14.1	0.018	0.037	5.42	80	4.30	9.18	17.5	0.0118
Ho	0.616	0.060	0.132	2.41	0.08	15.3	0.018	0.035	5.50	120	4.18	7.55	16.8	0.0119
Er	0.640	0.079	0.117	2.22	0.09	18.8	0.018	0.067	5.54	200	3.78	4.35	15.5	0.0122
Tm	0.644	0.101	0.104	2.00	0.10	21.5	0.018	0.102	4.00	300	3.36	2.58	14.2	0.0124
Yb	0.635	0.125	0.094	1.79	0.11	23.2	0.018	0.130	3.02	490	2.96	1.59	13	0.0126
Lu	0.617	0.149	0.085	1.59	0.12	24.1	0.018	0.190	2.00	632	2.59	1.02	10	0.0127
Ga	0.3	0.278	0.582	0.858	2.0	1.0	2	0.14	0	0	1.5	1.5	0.2	0
Cr	0.582	7.97	0.150	4.70	6.8	22.0	20	2.9	0	0	0.0029	380	0.2	0
Co	1.48	16.6	0.208	8	1.2	2.0	5.0	1.9	0	9	40	45	0.17	0
Ni	5.96	7.35	1.73	6.12	1.75	1.2	45	6.8	0	0	0.1	0.1	0.4	0
Cu	0.993	0.043	0.949	0.144	0.2	1.0	0.42	1.46	0	0	5	5.8	0.28	0
Zn	3.56	8.24	0.088	1.6	5.0	3.7	2.6	0.48	0	0	20	27	0.2	0
V	1.0	0.737	0.062	3.93	1.5	3.5	2	7.8	5.94	0	0.1	0.1	0.2	0
Sc	14.7	1.47	0.012	8.66	17.0	5.9	2	1.4	1.64	60	0.0001	50	0.22	0

Partition coefficients for Plag (Plagioclase), Cpx (clinopyroxene), and Opx (orthopyroxene) were calculated in the same manner as Bédard (2005; cf Fig. 6), and are appropriate for a temperature of 850 °C, An_{30} plagioclase, a melt SiO_2 of 60 wt% and/or a melt MgO of 3.5 wt%. Values for other minerals were compiled from the literature and will be presented elsewhere (Fig. 6). Biot, biotite; Magn, magnetite; Ilmen, ilmenite; Titan, titanite.

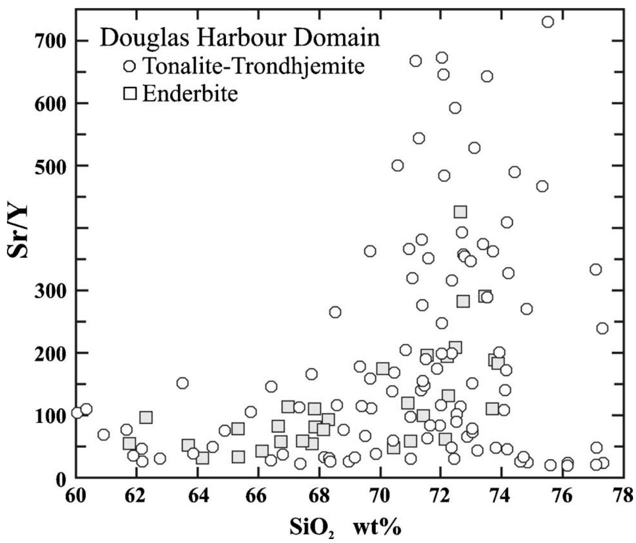

Fig. 5. Sr/Y vs. SiO_2 diagram showing tonalites, trondhjemites, and enderbites (pyroxene–tonalites) from the Douglas Harbour Domain. Note the overall trend of increasing Sr/Y as SiO_2 increases.

(*s.l.*) to andesitic mantle wedge melts (Feng and Kerrich, 1992; Kamber et al., 2002; Kleinhanns et al., 2003). However, andesites are a subordinate lava type in Archaean greenstone belts (see Section 2.9), and it seems implausible to attribute a fractionation origin to the dominant component of Archaean crust (TTGs), when its putative parental

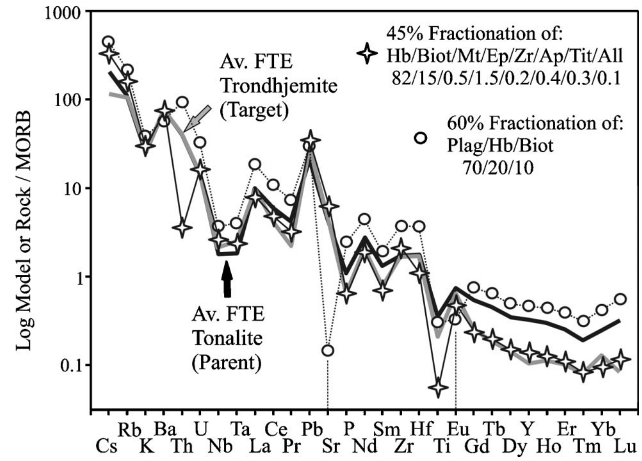

Fig. 7. Multi-element trace element profiles normalized to normal MORB (mid-ocean-ridge basalt: Sun and McDonough, 1989) for average tonalite and trondhjemite from the Eastern Faribault–Thury Complex. Two fractionation models are shown. The circles + dotted line shows results of 60% fractionation of a plagioclase + hornblende + biotite assemblage, while the stars with filled line show results for 45% hornblende-dominated fractionation. Plag, plagioclase, Hb, hornblende; Biot, biotite; Mt, magnetite; Ep, epidote; Zr, zircon; Ap, apatite; Tit, titanite; All, allanite. The prominent negative Th anomaly is caused by the extremely high D for Th in allanite. It is possible that in nature, allanite crystals may not be able to scavenge enough Th from the surrounding melt to satisfy its appetite for this element. The very large negative Ti anomaly results from use of an ${}^{\text{hornblende/melt}}D_{\text{Ti}}$ value of c. 4. Although this value seems appropriate for melts of 60% SiO_2 (Fig. 6), there is considerable scatter, and the value applicable to TTG differentiation could be somewhat lower.

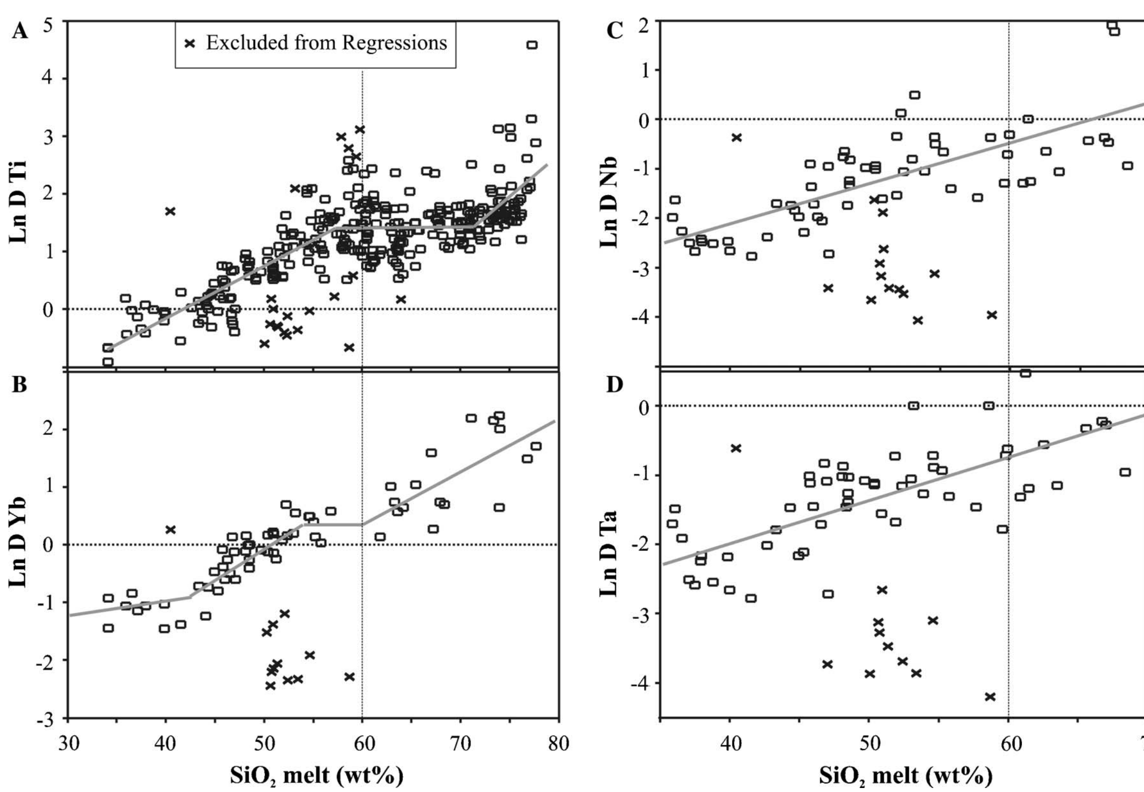

Fig. 6. Example of methodology used to parameterize D-data, shown here for Ti, Yb, Nb, and Ta in amphibole, using data from the literature. The complete REE profile at 60% SiO_2 was smoothed using the Lattice Strain Model of Blundy and Wood (1994), and results are given in Table 1.

magma is so uncommon. Nor are the huge volumes of amphibole + garnet cumulates expected from such a fractionation process observed (Smithies, 2000; Condie, 2005). In addition, a continuous magmatic flux would be predicted from a continuously operating arc source, rather than the episodic TTG pulses that are observed. For example, Whalen et al. (2004a) estimated that 20,000 km^3 of melt was emplaced in less than 5 Ma in the Lewis Lake Batholith of Ontario; far too much for an origin from a subduction zone. Furthermore, isotopic signatures and the abundance of inherited zircon cores in many TTG suites (McCulloch and Wasserburg, 1978; Gariépy and Allègre, 1985; Shirey and Hanson, 1986; Hill et al., 1989; Stern et al., 1994; Ridley et al., 1997; Leclair et al., 2001; Peck et al., 2001; Tomlinson et al., 2003; Whalen et al., 2002, 2004a) imply a major role for continental crustal recycling, rather than a purely fractionation origin.

2.9. Archaean plate tectonics?

Application of either the adakite or subduction zone fractionation models to the genesis of Archaean TT suite magmas require the existence of subduction zones and plate tectonic processes. In addition to the more specific points made above, there are general arguments against the attribution of modern plate-tectonic environments to Archaean assemblages. Specifically, most Archaean cratons do not display the structural, sedimentological, or metamorphic characteristics of Phanerozoic active margins (Kröner, 1991; Choukroune et al., 1995; Hamilton, 1998; Bleeker, 2002; Bédard, 2003; Bédard et al., 2003; Van Kranendonk et al., 2004; Stern, 2005). Accretionary/collisional orogens should be characterized by thrust-and-fold belts, reworked passive margin sequences, ophiolites, blueschists, high-pressure belts, accretionary prisms, and mélanges, of which there are no obvious, unambiguous examples in Pre-2.6 Ga Archaean greenstones (e.g., Goodwin, 1981, 1996; Schafer and Morton, 1991; Bickle et al., 1995; Hamilton, 1998; Zhai et al., 2002; McCall, 2003; Stern, 2005). Many greenstone belts that have been interpreted as collages of allochtonous accreted oceanic terranes, show compelling evidence for ensialic eruption and conformable stratigraphic contacts (Goodwin, 1981; Arndt, 1999; Green et al., 2000; Bleeker, 2002; Ayer et al., 2002; Thurston, 2002; Sproule et al., 2002; Bolhar et al., 2003; Tomlinson et al., 2003). Flysch and molasse deposits, which should be inevitable by-products of orogenesis, are also rare or absent (e.g., Lowe, 1982; Hamilton, 1998), and tend to be restricted to the 'late' history of any given craton (e.g., Davis et al., 1990; Hickman, 2004), when progressive rigidification and cooling of the crust allowed a transition towards more familiar, uniformitarian environments. The archetypal products of modern continental arcs, andesites, and basaltic andesites (e.g., Kelemen et al., 2004a), are largely subordinate to tholeiitic basalts in Archaean greenstone belts (e.g., Goodwin, 1981, 1996; Ayres and Thurston, 1985; Condie, 1986; Laflèche et al., 1992; Kerrich et al., 1999; Ayer et al., 2002; Blake et al., 2004). Although the proportion of calc-alkaline facies in Archaean greenstone belts is similar to that seen in primitive oceanic arcs (Miyashiro, 1974), the relative scarcity of Archaean andesites, and the intimate association with 'plume' facies such as komatiites and tholeiites, seems inconsistent with the attribution of an overall arc affinity to Archaean granite–greenstone terranes. Finally, the close association of coeval 'arc' and plume-derived magmas requires extremely complex tectonic and geodynamic scenarios, involving episodic terrane accretion, opening of slab windows and intermittent plume activity (e.g., Wyman et al., 2002). Given the scale of most greenstone belts (Fig. 3), these scenarios appear overly intricate (Hamilton, 1998).

In conclusion, it seems that the evidence supporting an arc environment for the Archaean TTG suite and the granite–greenstone terranes is not as strong as is generally believed, suggesting that alternative hypotheses should be considered.

3. Crustal cannibalism above large archaean plumes

3.1. Oceanic Plateaux

The principal alternative to the slab-melting model for generating the TTG suite is anatexis of: (1) the base of thick basaltic plateaux, (2) of tectonically thickened oceanic crust, or (3) of foundered portions thereof (Maaløe, 1982; Kröner, 1991; Kay and Kay, 1991; Atherton and Petford, 1993; Muir et al., 1995; Dirks and Jelsma, 1998a,b; Smithies, 2000; Conrey et al., 2001; Zegers and van Keken, 2001; Chung et al., 2003; Bédard et al., 2003; van Thienen et al., 2004a,b). Such models are compatible with the phase equilibrium and trace element requirements for TT genesis by moderate- to high-pressure metabasite anatexis ($P > 1.5$ GPa, reviewed in Moyen and Stevens, 2005). Oceanic plateaux are thought to form above major mantle upwellings (Coffin and Eldholm, 1994; Saunders et al., 1996), of which the largest Phanerozoic example is the 33–43 km thick Ontong-Java Plateau (e.g., Neal et al., 1997; Mann and Taira, 2004). The base of the Ontong-Java Plateau may have begun its transformation to eclogite (Vlaar et al., 1994; Saunders et al., 1996; Neal et al., 1997), which would explain why the plateau is not emergent. As shown by eroded/obducted examples in the Caribbean and South America, the internal structure of oceanic plateaux appears to be dominated by lavas, injected by increasing proportions of differentiated feeder dykes/sills towards their base (Saunders et al., 1996; Kerr et al., 1997, 1998). Since the crust is dominated by extrusive rocks, this affords the opportunity for uptake of H_2O and the acquisition of 'seafloor' O–C–H–Li isotopic signatures, with localized Fe-enrichment in the form of volcanic massive sulphide and ironstone deposition. Thus, low-temperature seafloor-alteration isotopic signatures, and the presence of metacumulate rocks, do not necessarily imply a ridge setting followed by subduction, as is generally proposed (e.g., Jacob et al., 1994; Schulze et al., 2000), but are equally consistent with oceanic plateaux settings.

Archaean basaltic plateaux may have been larger and thicker than Phanerozoic ones (Fyfe, 1978; Morgan and Phillips, 1984; Davies, 1993), because of the higher extents of melting that would result from a higher Archaean mantle potential temperature (Bickle, 1978, 1986; Sleep and Windley, 1982; Nisbet et al., 1993; Green and Falloon, 1998; Herzberg, 2004). In addition to magmatic thickening, mechanical interaction of adjacent oceanic plateaux may have led to peripheral tectonic thickening and terrane accretion or subcretion (de Wit et al., 1992; Kusky and Kidd, 1992; Kusky, 1998; de Wit, 1998; Dirks and Jelsma, 1998a,b; Tomlinson et al., 2003). The Ontong-Java plateau formed by major pulses at 120 and 90 Ma, with smaller pulses at 63 and 44 Ma (Tejada et al., 1996), suggesting a c. 20–30 Ma periodicity to plume-associated mantle melting/segregation events (cf. Prokoph et al., 2004). Given a higher magmatic flux, repeated ascent of hot magma, and a thicker metabasaltic pile, it is plausible to suggest that the base of Archaean oceanic plateaux may have begun to melt (Richter, 1985; Sandiford et al., 2004), generating a 1st generation of TT magmas (cf. Condie, 1984; Maaløe, 1982; Kröner, 1991). These early TT rocks could then be remelted by subsequent tholeiitic/komatiitic pulses to generate more voluminous and progressively more potassic TTGs. This type of repeated recycling of earlier anatectic products is required by the common presence of inherited zircon cores in Archaean TTGs, and their isotopic signatures and model ages (McCulloch and Wasserburg, 1978; Gariépy and Allègre, 1985; Hill et al., 1989; Bickle et al., 1989; Collins, 1993; Stern et al., 1994; Ridley et al., 1997; Whitehouse et al., 1998; Leclair et al., 2001; Tomlinson et al., 2003). The higher liquidus temperature of some Archaean magmas (komatiites: Herzberg, 2004; Parman et al., 2004) and the higher radiogenic heat productivity of Archaean crust and mantle (Lambert, 1976; Pollack, 1997; Sandiford et al., 2004), both would favour lower crustal melting. Buoyant felsic melts generated by such processes would tend to rise up into the denser basaltic carapace, leading to some type of partial convective overturn (Glazner, 1994; Goodwin, 1996; Collins et al., 1998; Bleeker, 2002; Bédard et al., 2003; Rey et al., 2003; Van Kranendonk et al., 2004).

3.2. Low-viscosity crust implies no mountains; no mountains implies no orogeny

The prerequisite to major crustal convective overturn is a partly molten, low-viscosity lower crust (Collins et al., 1998; Chardon et al., 1998; Mège et al., 2000). Low viscosities imply that Archaean continental crust should have been too weak to support high mountain ranges (Sandiford, 1989; Moser et al., 1996), and so, given the absence of mountains, the entire concept of Archaean 'orogenies' becomes problematic. A low-viscosity crust also implies the potential for lateral collapse of continental crust (Bailey, 1999), with felsic rocks flowing out over adjoining oceanic crust. Such a mechanism would generate shallowly dipping gneissic fabrics (e.g., Sandiford, 1989), and might explain the ubiquitous sub-horizontal lower-crustal reflectors seen in seismic profiles (e.g., Calvert and Ludden, 1999). Lateral flow would create a tensional environment in the proto-craton core, which would facilitate: (1) ascent and emplacement of TTG melts (Bédard et al., 2003), (2) delamination of lower crustal restites (Saleeby et al., 2003), and (3) partial convective overturn of the crust (Sandiford et al., 2004). The end result of such a process would be akin to shallow subduction, with the dense oceanic plate foundering, heating up, and melting (Bailey, 1999). However, the two phenomena are kinematically different, since in this case the laterally collapsing felsic crust plays the active role.

3.3. Geochemical tests relating metabasite to tonalitic magmas

An obvious 1st-order test of the hypothesis that TT suite magmas form by lower crustal metabasite anatexis is that, on average, the dominant felsic magma type (TT) can be generated by partial melting of the dominant mafic lithology (tholeiitic metabasalt). A series of simple equilibrium melting models were designed to investigate this hypothesis. The protolith used is the average amphibolite-grade metabasalt from the Douglas Harbour domain (av. MgO = 7 wt%), which makes up the north-eastern part of the Minto Block (Fig. 1; Bédard et al., 2003). Two types of tonalite occur in this domain, the older (c. 2.9–2.86 Ga) WFT tonalites, and younger (2.83–2.72 Ga) EFT tonalites (WFT and EFT = Western and Eastern Faribault–Thury Complex). The WFT tonalites are enriched in Ba–U–Th and REE in comparison with EFT tonalites. The trace element profiles of the 'parental' tonalites shown in Fig. 8 are averages of the more mafic tonalitic rocks in each suite (excluding a few, rare, lithologically distinctive diorites), and include fine-grained, hornblende-phyric, intraplutonic mela-tonalite dykes. Models were developed for different extents of melting and different residual assemblages. Partition coefficients (Table 1) were either taken from the literature (rutile, garnet, magnetite, ilmenite, biotite, allanite, and epidote) with some interpolation, or from recent parameterizations applied to appropriate melt and mineral compositions (clinopyroxene, orthopyroxene, plagioclase feldspar, Ca-amphibole: Fig. 6, Bédard, 2005).

The results for mafic to felsic granulite restites (Fig. 8C) show that plagioclase feldspar could not have been part of the residual assemblage to any extent (absence of negative Eu–Sr anomalies in FT tonalites). The younger EFT suite could not be modeled successfully with pure amphibolite residues (Fig. 8B), since these yield profiles with L/HREE ratios that are too low (cf. Rudnick and Taylor, 1986). Addition of garnet to the residual amphibolite assemblage improves the fit, but the L/HREE ratios are still too low

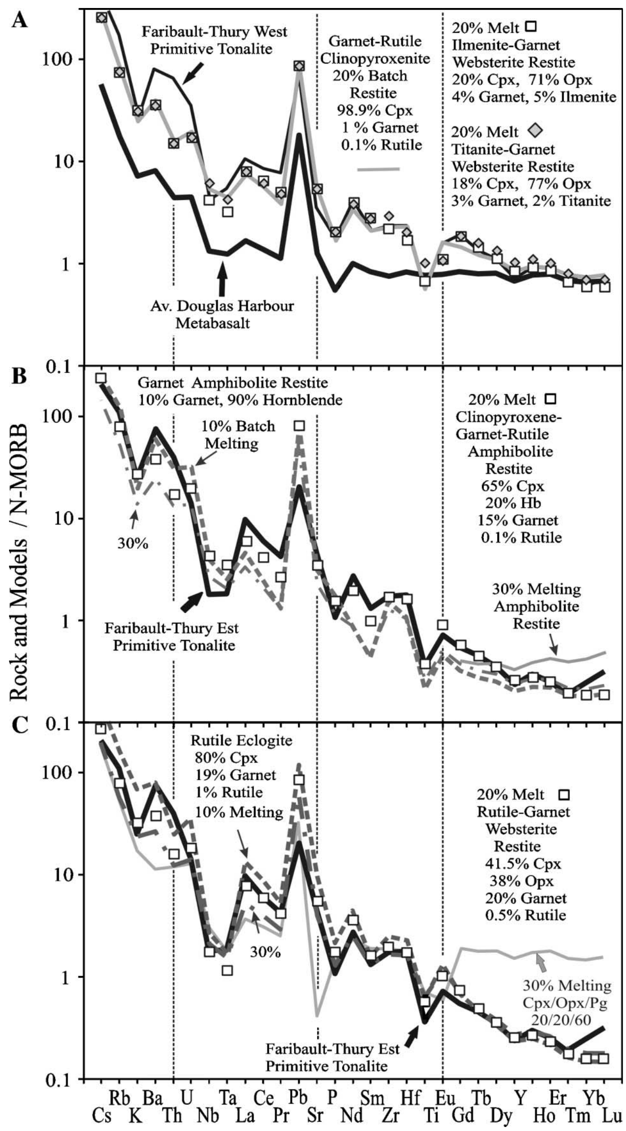

Fig. 8. Equilibrium melting models using the average tholeiitic metabasalt of the Douglas Harbour Domain (Fig. 2) as a parent (A), attempting to match the average Western (A) and Eastern (B and C) Faribault–Thury Complex tonalites for different restitic assemblages at different % melting.

(Fig. 8B). Addition of clinopyroxene and rutile to the garnet-amphibole restite assemblage improves the fit even more, and might represent an acceptable solution (Fig. 8B). However, the most successful models for EFT tonalite genesis are for rutile–eclogite or rutile–websterite restites (Fig. 8C). The requirement that garnet and rutile both be present implies pressures ⩾1.5 GPa (e.g., Moyen and Stevens, 2005). The older WFT tonalites were modeled (Fig. 8A) using garnet-bearing pyroxenite restites, with minor residual rutile, ilmenite or titanite. The models slightly under-estimate the LREE contents, and strongly under-estimate Ba–Th–U contents (Fig. 8A), suggesting that the average FT tholeiites may not be representative of the source of WFT tonalites. Despite a few caveats, these models do provide support for the plateau melting model, since they show that it is plausible to generate the dominant felsic parental melt of the FT complex by 20–30% melting of the most common mafic magma type (tholeiitic basalt), and that rutile, titanite or ilmenite-bearing garnet websterite to eclogitic restites are required (see Fig. 8).

The average FT metabasalt used in the models already has negative Nb–Ta anomalies, presumably caused by assimilation of older TT crust. It might be argued that the negative Nb–Ta anomalies in the derivative TT model melts are artefacts induced by using a protolith that itself has negative Nb–Ta anomalies. If the trace element profile of the basaltic protolith is straightened by increasing Nb from 3 to 7 ppm, and Ta from 0.16 to 0.3 ppm, then the average FTE tonalite shown in Fig. 8C can still be reproduced if the rutile eclogite restite contains 2% rutile, rather than 1%.

It has been argued that TTG melts generated by melting of lower crustal metabasites could not have acquired their high Mg#–Cr–Ni signatures for lack of an overlying mantle wedge (Martin and Moyen, 2002). The models of van Thienen et al. (2004a,b) imply that large delaminated slabs of lower crust have the potential to melt after detachment. This would increase the pressure of melting, helping to stabilize rutile-bearing eclogitic restites, and allow melts liberated from the delaminated slab to cross and react with mantle rocks during ascent, so increasing their Mg#, Cr, and Ni contents.

4. Fate of the restite

4.1. Restite delamination

If a 40 km thick TTG crust is generated by anatexis of metabasalt, then 80–200 km of eclogitic to pyroxenitic restite is generated (Rudnick, 1995; Wedepohl, 1995; Gao et al., 1998b; Rudnick et al., 2000; Arndt et al., 2002). Mass balance, isotopic and geophysical studies imply that these large volumes of clinopyroxene–garnet-rich restite are not present at the base of Archaean crustal sections (e.g., Drury et al., 1984; Arndt and Goldstein, 1989; Durrheim and Mooney, 1994; Ireland et al., 1994; Rudnick, 1995; Gao et al., 1998a,b; Rudnick et al., 2000; Niu and James, 2002; Rai et al., 2003). Because pyroxenite and eclogite are dense, numerical and analogue models imply that such restites would be unstable and should delaminate down into the mantle (Herzberg et al., 1983; Vlaar et al., 1994; Ducea and Saleeby, 1998a; Jull and Kelemen, 2001; van Thienen et al., 2004a,b). Eclogite suite xenoliths from kimberlites are largely of Archaean age (e.g., Pearson et al., 1995; Shirey et al., 2001; Barth et al., 2002a), and it has been proposed that many eclogite xenoliths are restites from anatexis of Archaean metabasalts (e.g., Ireland et al., 1994; Snyder et al., 1997; Rollinson, 1997; Rudnick et al., 2000; Barth et al., 2002a; Foley et al., 2002; Aulbach et al., 2002; Rapp et al., 2003). On the other hand, the O–C–H–Li isotopic signatures of SCLM eclogite xenoliths has been attributed to seafloor-metamorphism (e.g., Neal et al., 1990; Jacob et al., 1994; Schulze et al., 2000; Barth et al., 2001; Zack et al., 2003), which has generally led to the conclusion that they are relics of subducted oceanic crust (e.g., Helmstaedt and Doig, 1975; Neal et al., 1990; Jacob and Foley, 1999; Barth et al., 2001, 2002a,b,c). However, these seafloor metamorphic signatures could have been acquired in oceanic plateau environments and do not require the existence of subduction. Model restites and melts generated by batch melting of average FT metabasalt (see above, Fig. 8) are shown in Fig. 9. The model results imply that rocks with low Nb/Ta and Low Zr/Sm similar to most SCLM eclogites can indeed be generated as restites from anatexis of typical Archaean metabasalts (Fig. 9).

The ultimate fate of the negative crustal restite diapirs depends on their size, density, homogeneity and mineralogy; on the viscosity distribution of the mantle into which they penetrate; as well as on how differently-sized negative diapirs interact with each other and with the upwelling mantle. The largest of the negative diapirs are inferred to have moved rapidly (5–10 km/Ma: Vlaar et al., 1994; van Thienen et al., 2004b) and might have escaped from the SCLM (e.g., Rudnick et al., 2000; van Thienen et al., 2004b) to be recycled into deeper parts of the mantle, becoming components in the sources of younger ocean island or plateau basalt magmas (Hofmann and White, 1982; Christensen and Hofmann, 1994; Tatsumi, 2000; Albarède and van der Hilst, 2002; Kogiso et al., 2003). Partial delamination of restitic layers that retain some coherence might produce sloping mantle reflectors (e.g., Calvert and Ludden, 1999) that could be misidentified as fossil subduction zones (Fig. 10D, Hamilton, 1998, p. 18). In the next sections, I explore the possibility that delaminated restites might mix with the upper mantle, and the consequences thereof.

4.2. Factors influencing mixing of delaminated crustal restite and mantle

Theoretical arguments imply that a high viscosity contrast hinders mixing (e.g., Marshall and Sparks, 1984; Manga, 1996; du Vignaux and Fleitout, 2001; Dzwinel and Yuen, 2001). In the plateau melting model, generation of eclogitic crustal restite represents the culmination of a major pulse of mantle-derived magmatism, with essentially synchronous development of a depleted mantle root and a migmatized crust (Fig. 10). Given inefficient extraction of melt from crust and mantle restites, then it seems plausible that both restites might retain a small melt fraction (c. 1–5%) at essentially the same time (cf. Saleeby et al., 2003). Since the viscosity of mixed media is dominated by the melt fraction (Ji et al., 2004), then there should be little viscosity contrast between mushy crustal restite, and mushy mantle restite, and mixing might be very efficient in consequence.

Mixing would also be favoured by the episodic and potentially catastrophic (van Thienen et al., 2004b) nature of delamination events, since differently sized diapirs, with different viscosities, that move at different rates, might impinge in an irregular, chaotic way and disrupt one another.

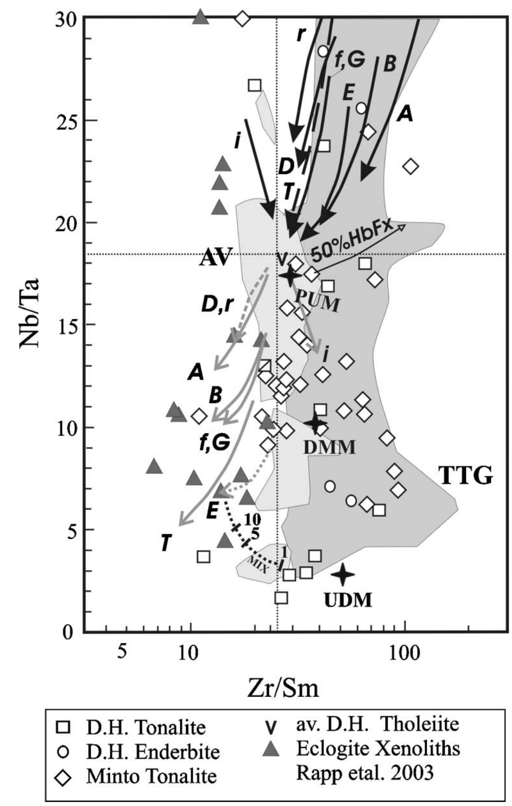

Fig. 9. Nb/Ta vs. Log(Zr/Sm) diagram adapted from Rapp et al. (2003). The grey TTG field and eclogite xenoliths are from Rapp et al. (2003). The pale grey field labeled AV is the field of Superior Province Archaean mafic volcanics from Rapp et al. (2003), complemented by data from the Douglas Harbour Domain (Madore et al., 1999). The open symbols show tonalites and mela-enderbites ($SiO_2 < 70\%$) from the Douglas Harbour domain (D.H.) and other Minto locales (Bédard, 2003). Note that these data extend offscale to higher Nb/Ta than shown here. The intersecting dashed lines show chondritic ratios, while the star marked 'PUM' is primitive upper mantle (Sun and McDonough, 1989). The star marked 'DMM' is depleted MORB mantle fromWorkman and Hart (2005), while the star marked 'UDM' is for ultra-depleted mantle from Bédard (1999) residual from c. 25% melting of PUM, which is used in the model shown in Fig. 13. The 'v' is the average metabasalt used in the modeling of Fig. 8. The bold black arrows show the melt trends (% melting increasing from 5 to 40%), produced in the different equilibrium melting models, while the grey arrows show the trend of the corresponding restites. Restite assemblages are: A: 100% Hb;. B: 65:15:20 Cpx:Hb:Gt; D: 80:19:1 Cpx:Gt:Rut; E: 80:20 Cpx:Gt. %; f: 98.9:1:0.1 Cpx:Gt:Rut; G: 20:20:60 Cpx:Opx:Pg; r: 41.5:38:20:0.5 Cpx:Opx:Gt:Rut; T: 18:77:3:2 Cpx:Opx:Gt:Titanite; i: 20:71:4:5 Cpx:Opx:Gt:ilmenite. Hb, Hornblende; Cpx, Clinopyroxene; Opx, Orthopyroxene; Pg, Plagioclase; Rut, Rutile; Gt, Garnet. The arrow trending to the top right labeled 50%HbFx shows the path of 50% fractionation of an hornblende-dominated assemblage (Fig. 7) from the EFT tonalite parent. The dotted line labelled 'MIX' at the bottom of the figure shows results of mixing residues of 40% crustal anatexis (curve 'E') with the ultra-depleted mantle residue (UDM). The numbers represent the % of crustal restite in the mixture.

In addition, if the delaminated root contains domains of high density (banded iron formation, massive sulphide), or low density (marble, metasediment, low-Fe amphibolite, tonalite, zones with abundant trapped melt), then differential movement of these domains would also stir the mixture (Ferrachat and Ricard, 1998; Jellinek et al., 1999; Farne-

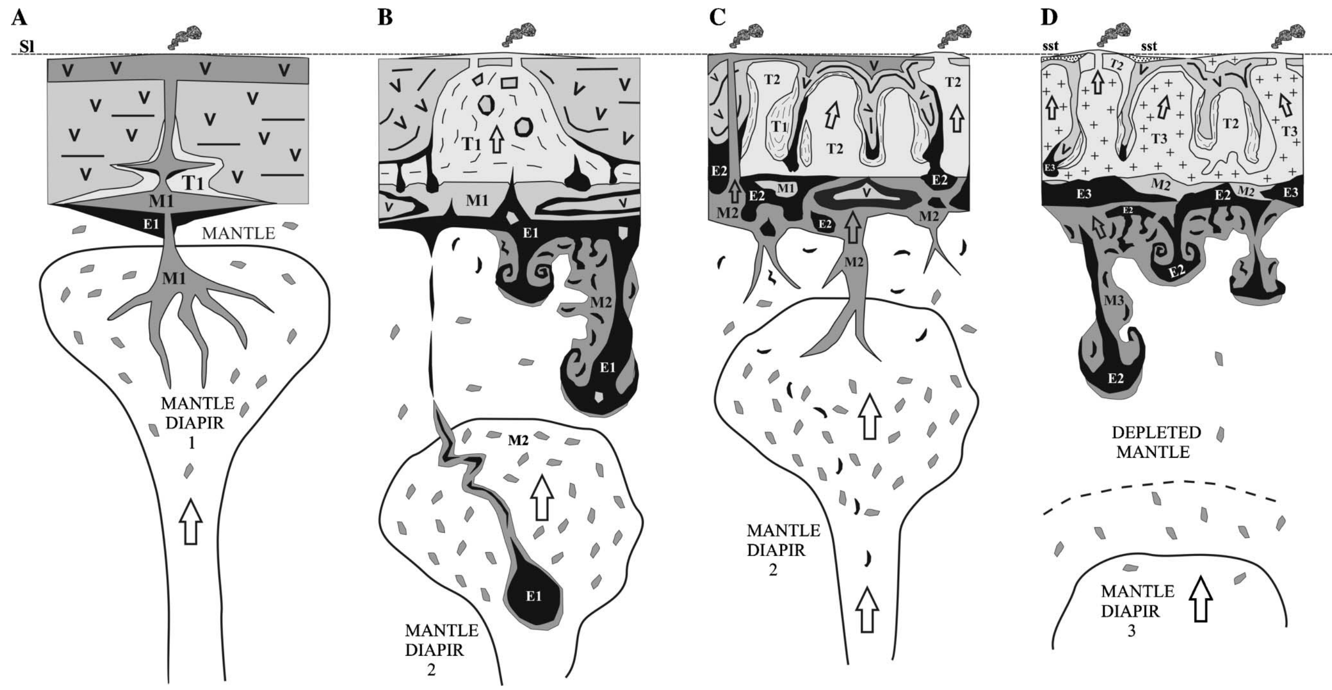

Fig. 10. (A) Cartoon illustrating the catalytic delamination-driven tectonomagmatic model discussed in the text. A large mantle plume releases melt (M1) that constructs a thick volcanic crust. Underplating magma causes melting at the base of the crust to form a 1st generation of tonalitic melt (T1) with complementary eclogitic to pyroxenitic restites (E1). (B) As M1-magmatism wanes, the underplated melt layer cools and crystallizes. Buoyant tonalitic melt (T1) rises into the volcanic carapace, initiating a 1st cycle of partial crustal convective overturn. Dense restites and cumulates (E1) delaminate into the mantle. Large bodies of E1 travel fast and escape into the deep mantle, and may guide ascent of mantle diapirs. Smaller delaminated bodies mix into the shallow upper mantle and trigger the formation of a 2nd generation of mantle melt (M2). The M2 label here represents melt-enriched domains. (C) The 1st generation crustal restites are largely destroyed as M2 melts are generated, collect and ascend. New melt from a 2nd mantle diapir also contribute to M2. Eruptions of M2 fill troughs in the surface. Mantle melt (M2) that underplates the crust generates a 2nd generation of tonalite melt (T2) by melting relicts of lava (v) and of the underplated M1 magma, yielding a 2nd generation of restites and cumulates (E2). Older tonalites (T1) are extensively remobilized at this time, and also contribute to T2. The voluminous T2 tonalites are buoyant and trigger a 2nd cycle of partial crustal convective overturn. (D) As M2-magmatism wanes, the underplated layer cools and crystallizes. The restites and cumulates (E2) delaminate into the mantle, triggering the formation of a 3rd generation of mantle melts (M3), and destroying the 2nd generation restites. Melting of underplated M2 melt and relict lavas generate a 3rd generation of tonalitic to granodioritic melt (T3), also yielding a 3rd generation of restites and cumulates (E3). Older tonalitic rocks (T1 and T2) are extensively remobilized and represent the dominant part of T3. The voluminous T3 tonalites/granodiorites are buoyant and trigger a 3rd cycle of partial convective overturn in the crust. Tonalitic bodies that protrude above sea level (sl) are eroded to form sandstones (sst) and conglomerates (cf. Bleeker, 2002).

tani et al., 2002) and contribute to the disruption of the negative diapirs, much as the rotation of phenocrysts hybridizes mingled melts (e.g., Kouchi and Sunagawa, 1985). Lateral and vertical variations in the viscosity structure of the mantle and negative crustal restite diapirs might also result in complex mixing scenarios (cf. Kumagai, 2002). The evidence from exposed slab/mantle contacts suggests extensive mechanical and chemical interaction caused by shear heterogeneities (e.g., Bebout and Barton, 2002); while field evidence from syn-kinematic intrusions in lower ophiolitic crust (Bédard et al., 2000), and from lavas and feeder dykes (Perugini et al., 2003), both suggest that hybridization of partially molten bodies subject to shear deformation is fast and easy.

5. Consequences of mixing crustal and mantle restites

5.1. A catalytic delamination-driven model

Mantle melt productivity (especially during fractional melting) decreases markedly when the easily fusible, high-Ca–Al phases (e.g. garnet and clinopyroxene) are exhausted (e.g., Bowen, 1928; Presnall et al., 1979; Dick et al., 1984; Maaløe, 1985; Wasylenki et al., 2003). Thus, as a large Archaean plume rises, decompression-driven melting should tail off when clinopyroxene and/or garnet are exhausted. What then will be the consequence of physically mixing crustally derived garnet and clinopyroxene into this harzburgitic residue (Vlaar et al., 1994; Ireland et al., 1994; Yaxley and Green, 1998; Nielsen et al., 2002; Simon et al., 2003; Gao et al., 2004)? Since clinopyroxene and garnet typically contribute 30–70% of the melt component during basaltic melt genesis (e.g., Johnson and Dick, 1992; Niu, 1997; Walter, 1998; Bizimis et al., 2000), then each km^3 of delaminated pyroxenite or eclogite that is blended into a depleted harzburgite generates a refertilized lherzolitic mantle which could potentially yield 1–3 km^3 of new melt. Because heat is needed for the phase change (latent heat of melting), it seems likely that a catastrophic and widespread mixing event involving delamination of a thick crustal restite layer might lead only to thermal death. On the other hand, if negative diapirs are widely spaced, and are mixed into a larger volume of mantle, then thermal diffusion might be able to keep pace and generate a large volume of new basaltic melt. Lower crustal delamination would induce a compensatory mantle upwelling and so yield additional increments of mafic melt by decompression (Vlaar et al., 1994; van Thienen et al., 2004a,b).

Admixture of a pyroxenitic/eclogitic component has been investigated theoretically and experimentally, and has been shown to result in increased melt productivity (Yaxley and Green, 1998; Pickering-Witter and Johnston, 2000; Yaxley, 2000; Hirschmann et al., 2003; Kogiso et al., 2003). Melt production is concentrated at the interface between the fertile xenolith and the host mantle, and orthopyroxenite-enriched reaction rims may form (Yaxley and Green, 1998). The composition of the melt is strongly dependent on the bulk composition of the admixed pyroxenitic component (Kogiso et al., 2004). Addition of fertile 'basalt' to mantle peridotite yields low-Mg# melts (Yaxley, 2000). Since an eclogitic/pyroxenitic restite from metabasite anatexis would typically have an Mg# higher than that of its original basalt, then addition of high-Mg# crustal restite to depleted mantle might be expected to yield higher-Mg# melts. Such high-Mg#, 2nd-stage melts would be rather buoyant as a result, and tend to rise and either erupt, or underplate the nascent tonalitic crust. Underplating of felsic rocks by mafic melt is an efficient way to induce anatexis both of the felsic lithologies (e.g., Wyllie et al., 1976; Huppert and Sparks, 1988; Fountain, 1989; Petford and Gallagher, 2001; Koyaguchi and Kaneko, 1999; Annen and Sparks, 2002), and possibly of previously unmelted or newly underplated basalt (Rollinson and Windley, 1980; Rudnick and Taylor, 1986; Annen and Sparks, 2002), and so would generate new increments of tonalitic melt + pyroxenitic to eclogitic restite. This 2nd generation restite, if thick enough, would also be mechanically unstable and should delaminate into the mantle (Fig. 10), where it might trigger renewed melting, and so on... (cf. Herzberg et al., 1983; Vlaar et al., 1994; Van Kranendonk et al., 2004). Viewed another way, CaO and Al_2O_3 occur in easily fusible phases (clinopyroxene and garnet) in the mantle, and so are incompatible, yielding buoyant melt. Conversely, these elements are compatible in the crust, stabilizing dense liquidus or restite phases (clinopyroxene, garnet, hornblende, epidote, titanite...) that tend to founder back into the mantle. This contrast suggests the possibility that the Ca–Al component (eclogite/pyroxenite) represents a catalyst for coupled differentiation of the crust and mantle in the Archaean.

5.2. Phase equilibrium and thermodynamic constraints

The detailed mechanisms by which eclogitic restites react with the upper mantle is probably best investigated experimentally. Nonetheless, some insights may be gained by consideration of basic phase equilibrium relationships, and by thermodynamically based models (e.g., Boudreau, 1999; Ghiorso et al., 2002). The former is illustrated with a 2 GPa forsterite–anorthite–quartz liquidus surface diagram from Liu and Presnall (1990), in the CMAS system (Fig. 11). During partial melting, extraction of voluminous eutectoid melt enriched in the anorthite component (CaO and Al_2O_3) will leave a depleted restite (S2), where the amount of melt of composition $L2 = a/a + b$, by the lever rule (Fig. 11B). If melting is near-fractional, a large temperature increase will be needed before much more melt can be extracted from this depleted mantle restite. What then will be the consequences of mechanically adding eclogitic restites from crustal metabasite anatexis? Garnet and clinopyroxene plot off the join, but are located towards the anorthite pole, and a hypothetical mixing line (heavy dashed line labelled 'Mix') is drawn between mantle and

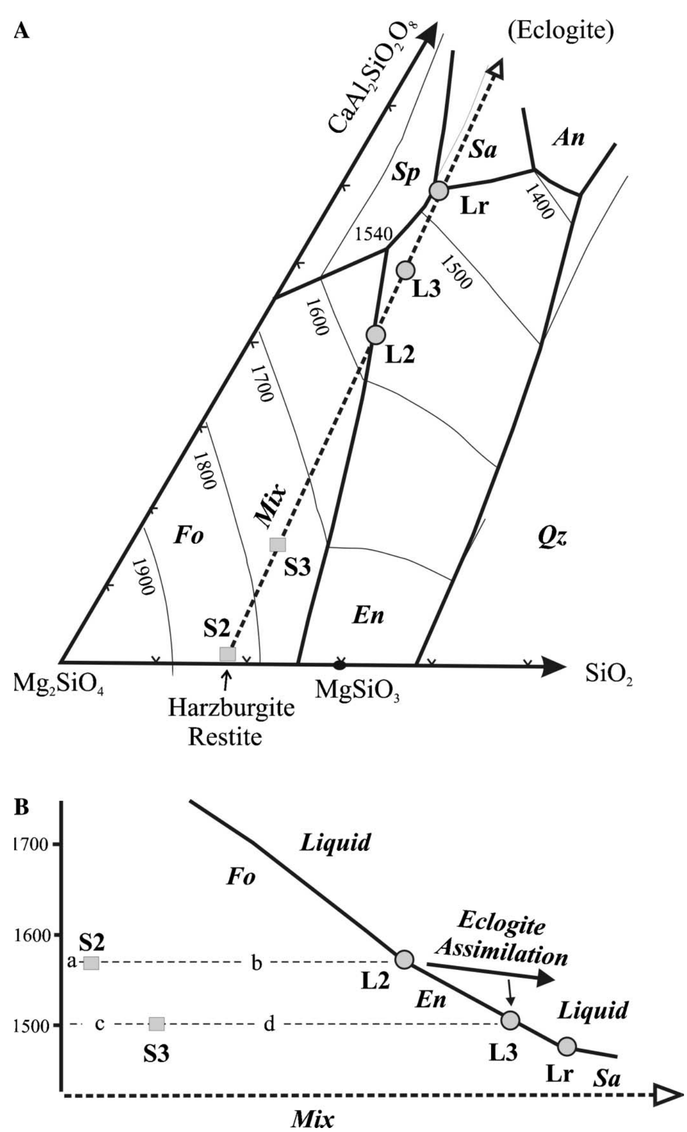

Fig. 11. (A) Liquidus phase diagram adapted from Liu and Presnall (1990). Fo, forsterite; En, enstatite; Sp, spinel; Sa, sapphirine; An, anorthite; Qz, high quartz. Heavy curves are phase boundaries, light lines are isotherms labelled in °C. S2 and S3 = hypothetical mantle harzburgite restite and refertilized lherzolite, respectively. L2 and L3 = liquids in equilibrium with S2 and S3, respectively. Lr = liquid at the $En = Sa$ reaction point. In (B), a section is shown along mixing line 'Mix.'

crustal restites. A cross-section is drawn along this mixing line in Fig. 11B. Adding cool eclogite shifts the bulk composition to S3, and necessarily leads to an increase in the proportion of melt ($=c/c+d$). Another way to visualise this is to consider the effect of dissolving clinopyroxene and garnet (enriched in CaO and Al_2O_3) into a melt saturated in forsterite + enstatite (e.g., L2). Adding such components will pull the melt composition off the liquidus surface (compositional undersaturation) and lead to dissolution of forsterite and eventual precipitation of enstatite, and contribute to the increase in orthopyroxene/olivine mode seen in Archaean-aged subcontinental lithospheric mantle. Because heat is consumed during melting, the system will cool, but because of the steep slope of the liquidus surface (Fig. 11B), then assimilation of a relatively cold eclogite will still lead to significant melting.

Table 2
Partition coefficients used to model mantle melting

	Cpx	Opx	Oliv.	Cr-Sp
Cs	0.0014	0.0108	0.0013	0.0001
K	0.0029	0.0108	0.0013	0.0001
Rb	0.0021	0.0108	0.0013	0.0002
Ba	0.0007	0.0146	0.0013	0.0005
Th	0.0062	0.0015	0.0009	0.001
U	0.0047	0.0058	0.0006	0.001
Nb	0.0045	0.0058	0.0008	0.01
Ta	0.0115	0.0465	0.0084	0.01
La	0.0520	0.0012	0.0002	0.0006
Ce	0.0776	0.0020	0.0004	0.0006
Pr	0.110	0.0034	0.0008	0.0006
Pb	0.0164	0.0050	0.0013	0.0006
Sr	0.0916	0.0050	0.0013	0.0006
P	0.0427	0.0411	0.00005	0.0006
Nd	0.148	0.0054	0.0012	0.0006
Sm	0.220	0.0118	0.0026	0.0006
Zr	0.0549	0.0185	0.0065	0.015
Hf	0.153	0.0360	0.0060	0.015
Ti	0.288	0.1405	0.0132	0.125
Eu	1.203	0.0163	0.0051	0.0006
Gd	0.276	0.0215	0.0050	0.0006
Tb	0.296	0.0285	0.0067	0.0011
Dy	0.310	0.0371	0.0089	0.0015
Y	0.315	0.0434	0.0106	0.002
Ho	0.316	0.0468	0.0115	0.0023
Er	0.316	0.0573	0.0143	0.003
Tm	0.311	0.0683	0.0172	0.0038
Yb	0.303	0.0794	0.0203	0.0045
Lu	0.293	0.0903	0.0233	0.0045
Ga	0.272	0.278	0.103	4
Cr	7.3	2.8	0.69	500
Co	0.798	1.122	3.20	4
Ni	0.0388	1.597	6.75	10
Cu	0.263	0.0432	0.05	1
Zn	0.243	1.122	0.968	4
V	3.1	0.194	0.15	10
Sc	7.35	0.559	0.170	0.1

D values for mantle melting based on parameterizations of Bédard (2005) for olivine. D values for orthopyroxene and clinopyroxene were calculated in a similar manner, assuming a temperature of 1300 °C, and MgO in the melt of 13 wt%, and a clinopyroxene tetrahedral Al content of 0.095. Chrome-spinel D values from Bédard (1999).

The mechanical introduction of eclogitic crustal restites into a solidus-temperature depleted mantle restite was also simulated using the PELE modeling software of Boudreau (1999, version 6XX), an adaptation of MELTS (Ghiorso et al., 2002). The models were executed as equilibrium crystallization experiments, since this is the inverse of equilibrium melting. As a starting point, I used an experiment (#2) on a depleted peridotite by Laura Wasylenki et al. (2003). At $P = 1$ GPa, $T = 1330$ °C, for QFM ~ -2, this experiment contains 10% glass (MgO = 12.8%), 67.1% olivine and 22.9% orthopyroxene, and is therefore at a temperature above clinopyroxene-out and spinel-out. The bulk composition was reconstructed from the modes and mineral analyses (#2, Table 3), and was run in PELE as a test of the thermodynamic model (Fig. 12). The model was run as an equilibrium crystallization experiment, dry, at constant pressure, and yielded 13.9% liquid (13.1% MgO), 64.4% olivine, 0.9% spinel, and 21.2% orthopyroxene. Since dissolution of Cr into pyroxene is not considered in PELE, this is considered a satisfactory reproduction of the original experimental data. If the system is allowed to crystalllize at equilibrium, the liquid dwindles to <1% (6.5% MgO) by 1255 °C, after crystallizing 6% orthopyroxene, 4% Cr-spinel, 8% clinopyroxene, and resorbing 5% olivine. Wasylenki et al. (2003) estimated the solidus at somewhere

Table 3
Starting compositions for crystallization–assimilation simulations

	2	2R	R2R	FTER	C2Rw
SiO_2	45.16	44.79	45.02	46.82	44.88
TiO_2	0.04	0.02	0.13	1.11	0.98
Al_2O_3	2.39	1.25	2.64	14.19	13.91
Fe_2O_3	0.00	0.00	0.00	0.00	2.73
FeO	8.23	8.30	8.86	13.47	8.92
MgO	41.59	44.09	40.36	9.28	12.89
CaO	2.13	1.13	2.41	13.07	14.81
Na_2O	0.06	0.02	0.18	1.56	0.58
K_2O	0.01	0.01	0.03	0.19	0.21
Cr_2O_3	0.39	0.40	0.36	0.05	0.00
H_2O	0.00	0.00	0.00	0.00	0.08
Glass	10.0	2.17			
Olivine	67.1	72.93			
Orthopyroxene	22.9	24.62			
Clinopyroxene				80	50.07
Magnetite					3.97
Garnet				19	33.05
Rutile				1	0.98
Albite					4.89
biotite					2.01
Corundum					5.04

2, reconstructed bulk composition of experiment #2 (Wasylenki et al., 2003) at F = 0.1. 2R, normalized residue of #2, after loss of 8% of the melt. R2R, refertilized version of 2R (0.1 × FTER + 0.9 × 2R). FTER, residue from 20% melting of the average Faribault–Thury tholeiite calculated by mass balance. C2Rw, composite wet contaminant. Biotite, phlogopite: annite 60:40; clinopyroxene, diopsite:hedenbergite 82.6:17.4; garnet, pyrope:grossular:almandine 55:17:28. Composition of clinopyroxene and garnet are similar to composition of minerals in restites from metabasite anatexis determined by Barth et al. (2002a).

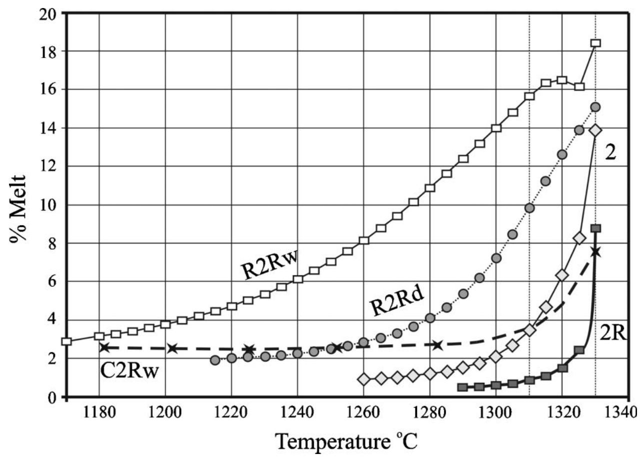

Fig. 12. Results of thermodynamic models showing how the % melt changes with temperature. Isobaric experiments: 2, equilibrium crystallization/melting experiment corresponding to the reconstructed bulk composition of experiment #2 from Wasylenki et al. (2003) at F = 0.1; 2R, normalized residue of #2, after loss of 8% of the melt; R2R, refertilized version of 2R ($0.1 \times FTER + 0.9 \times 2R$), where FTER = residue from 20% melting of the average Faribault–Thury tholeiite (Table 3). R2Rw and R2Rd are wet (0.1 wt% H_2O) and dry experiments, respectively; C2Rw, isenthalpic coupled assimilation/crystallization experiment, where 10gr of composite wet contaminant C2Rw (Table 3) is added at each step.

between 1250 and 1270 °C, in agreement with the PELE model.

To generate the model mantle restites used in the next runs, only 2% glass was retained in the mantle mixture, using the same mineral compositions from experiment #2 (i.e., 2% glass, 67.1% olivine, and 22.9% orthopyroxene). This simulates the retention of a small amount of equilibrium melt from the restite. Crystallizing this bulk composition (#2R, Table 3) in PELE, at the same conditions as above, yields only 8.8% melt (13.8% MgO) at 1330 °C, which decreases very rapidly with cooling, with <1% liquid (11% MgO) remaining by 1310 °C (Fig. 12).

Admixture of eclogite to #2R was done in two different ways. First, the composition of the crustal restite was calculated by extracting 20% of the Faribault–Thury Est parental tonalite composition (as determined from the distribution of data on variation diagrams), from the inferred protolith, the average FT tholeiite. This crustal restite (FTER) was added to #2R in a 1:9 proportion, to generate a refertilized peridotite #R2R, which was run in PELE under both wet (0.1% H_2O) and dry conditions. In the dry model (#R2Rd), mantle #R2R was allowed to crystallize starting at 1330 °C. The initial melt content was 15.1% (Fig. 12), significantly higher than the #2R melt content, but was not much less magnesian (12.8% MgO). In marked contrast to the #2R experiment, #R2R still contains 9.8% melt (11.3% MgO) at 1310 °C, the temperature at which #2R was almost completely solid. In addition, #R2R continued to crystallize beyond 1215 °C, where 1.91% melt still remained (4.3% MgO), after crystallizing 8.2% clinopyroxene, 4.9% orthopyroxene, 3.1% spinel, and resorbing 3% olivine.

The wet model (#R2Rw) only differs by having 0.1 wt% water, which lowers the mantle solidus temperature. The PELE simulation also reproduces this effect, since the initial conditions (1330 °C) yield (Fig. 12) a slightly higher proportion of melt 18.4% (13% MgO). By 1310 °C, 15.7% melt (12.1% MgO) remain. The run was continued to 1170 °C, where 2.9% melt remain (4.8%MgO) after crystallization of 8.6% clinopyroxene, 6.4% orthopyroxene, 3.9% spinel, and resorption of 3.3% olivine. What these models imply is that a refertilized mantle generated by mixing in an eclogitic restite can generate abundant melt.

If the latent heat effect is neglected, then addition of a 900 °C contaminant to a 1330 °C host mantle in a 1:9 proportion yields an equilibration temperature of 1287 °C, which gives 4.7% and 12% melt in the R2Rd and R2Rw experiments. These values are maxima, since energy (latent heat) will be consumed to effectuate the solid–liquid phase transition. To take advantage of PELE's capacity to do thermodynamically constrained coupled assimilation-crystallization models, I generated a model 'contaminant' constituted of simplified minerals (4.89% albite, 2.01% biotite (Phl_{60}, Ann_{40}), 50.07% clinopyroxene (Di_{83}), 33.05% garnet (Pyr_{55}, $Gross_{17}$, Alm_{28}), 5.04% corundum, 0.98% rutile, 3.97% magnetite); and which is compositionally similar to the calculated FTER (Table 3). The model contaminant simulates an eclogitic restite generated at c. 900–1100 °C, with the compositions of clinopyroxene and garnet being similar to those analyzed by Barth et al. (2002a) at 1.8 GPa and 1000–1040 °C. The added albite, corundum and magnetite were included to supply Na_2O, Al_2O_3, and Fe_2O_3, which are not considered by the PELE solid contaminant subroutine. Minor biotite was added to supply K_2O and H_2O. The model contaminant was added in 10 gr/step increments during a crystallization experiment (#C2R: Table 3). Only one simulation is shown for comparison to the #2 and #2R experiments in Fig. 12. The contaminant was attributed a temperature of 900 °C, which is the minimum needed to generate abundant tonalitic melt; but the assemblage contained 0.08% water. The objective was to see if addition of large amounts of cold contaminant would cause the system to freeze out, or whether addition of Al_2O_3, CaO. FeO, Na_2O, K_2O, and water induces enough compositional understauration to keep the system molten. The model indicates that at 1310 °C, about 4% melt (MgO 11.6%) remains, while at 1181 °C, 2.56% melt remained (3.7% MgO).

The extensive depression of the solidus shown in all of these simulations implies that addition of an eclogitic or pyroxenitic crustal restite to a near-solidus temperature restitic harzburgite will generate extensive amounts of melt, whether or not temperatures are buffered, and whether or not water is present. While latent heat is an important factor, its effects are too small to prevent melting if the admixed eclogite is a small fraction of the mixture.

5.3. Paradox redux

Such a catalytic model could perhaps resolve a number of troubling paradoxes about Archaean magmagenesis, mantle genesis, and tectonics, as follows:

(1) Because both mantle and crustal restites tend to have higher Mg# than their respective protoliths, then the mixed source should yield 2nd stage melts that have high Mg#, and leave a 2nd stage mantle restite with high Mg#. This may explain the unusually high Mg# of many Archaean SCLM xenoliths (Griffin et al., 2003; Herzberg, 2004). Since much of the interaction between foundered crustal restite and mantle restites occurs at shallow levels, then this could help explain why most SCLM rocks retain apparent spinel-facies trace element signatures (Canil, 2004).

(2) Reaction between delaminated clinopyroxene-rich material and a melt-bearing harzburgitic mantle restite might generate the excess orthopyroxene of some Archaean SCLM suites (Fig. 11). Field observations from the lower crust of the Bay of Islands Ophiolite (Bédard et al., 2000) indicate that clinopyroxene-rich rocks dissolve incongruently into a melt saturated in olivine + orthopyroxene, with the production of orthopyroxenitic reaction rims. Generation of excess orthopyroxene by reaction between 'eclogite' and mantle also has experimental support (Yaxley and Green, 1998), and websteritic mantle xenoliths have been interpreted to result from such interactions (Aulbach et al., 2002).

(3) The catalytic model accounts for the missing eclogitic root, since the eclogitic restite would be largely consumed by partial melting in the shallow mantle. The eclogitic component would cycle through the system several times in order to generate the appropriate geochemical signatures, so that instead of extracting 200 km of eclogitic restite as a single event, 20 km of eclogite may cycle through the system 10 times. Extensive shallow destruction/recycling of delaminated eclogitic cumulates and restites explains why the eclogitic xenolith suite now makes up <1% of the SCLM (Jacob, 2004). Only fairly large eclogite pods would survive such a process, which explains why eclogitic xenoliths are so abundant in kimberlite pipes which intersect them, yet are nearly absent from the dominant 'background' mantle.

(4) Repeated cycles of delamination, mantle upwelling and magmatism would reheat previously crystallized felsic crust, and near-total remelting might occur when voluminous high-temperature basaltic to komatiitic melts underplate older TTs (e.g., Wyllie et al., 1976; Huppert and Sparks, 1988; Fountain, 1989; Koyaguchi and Kaneko, 1999; Zegers and van Keken, 2001; Annen and Sparks, 2002). This could explain: (a) the existence of large volumes of high-temperature (>1000 °C) enderbitic melts (e.g., Bédard, 2003); (b) the common presence of inherited zircon cores in Archaean felsic plutons; and (c) lead to secular K-enrichment as the highly-incompatible elements build up in the crustal partial melts.

(5) Mixing of the crustal restites complementary to FT tonalite genesis into depleted mantle residues generates sources with sub-chondritic Nb/Ta and near-chondritic Zr/Sm ratios (dotted line marked 'MIX' in Fig. 9), that can yield basalts with such geochemical signatures, which could then remelt to generate low Nb/Ta high-Zr/Sm TTGs (cf. Rapp et al., 2003).

(6) Some of the less common Archaean magma types can be accounted for by variants of the delamination-hybridization scenario outlined above. (a) If undepleted metabasalt domains are entrained into the mantle during delamination of a larger eclogitic diapir (Moresi and Solomatov, 1998; van Thienen et al., 2004b), then melting of amphibolite (cf. Foley et al., 2002; van Thienen et al., 2004a), or fertile eclogite (Ducea and Saleeby, 1998b; Rapp et al., 2003), could yield tonalitic melts that would react with the surrounding mantle as it ascends, become enriched in Mg#, Cr, and Ni, and also lead to SiO_2 enrichment and generation of excess orthopyroxene in the SCLM (Kelemen et al., 1998). (b) Entrained metasedimentary or metavolcanic rocks might yield high-LILE melts or fluids when they heat up. Areas of the mantle and crust metasomatized by such LILE-enriched fluids could yield sanukitoids and shoshonites, or trigger shallow melting of surrounding, depleted harzburgite, potentially generating Archaean 'boninites' or hydrous komatiites (Kerrich et al., 1998; Parman et al., 2001; Smithies, 2002; Grove and Parman, 2004). (c) Involvement of delaminated VMS in the catalytic melting process may generate anomalously S-rich magmas that could lead to the development of Ni-sulphide ore deposits.

(7) The formation of Archean cratons and SCLM is roughly coeval (Pearson, 1999; Griffin et al., 2003), but occurs at different times (between 3.6 and 2.7 Ga) in different cratons (e.g., Goodwin, 1981, 1996; Windley, 1984). The diachroneity of cratonization is also explained by the catalytic model, since the processes by which cratonic crust and SCLM form could be triggered by any plume-like mantle instability of sufficient size. The main requirement is a magmatic flux sufficient to form a thick volcanic pile that can cannibalize its own base to yield gravitationally unstable pyroxenitic to eclogitic restites. Once begun, gravitationally driven mass movements (delamination) would trigger new pulses of mantle melting, and initiate the catalytic loop described above. In

such a delamination-driven tectonomagmatic model, the distribution of plutonic activity at shallow levels (mid-upper crust) would be controlled by the location and scale of lower crustal delamination events; and so upwelling zones need not be finger-like, but could also take the form of linear belts.

Continental and mantle evolution models are based largely on mass balance calculations and trace element ratios (e.g., McDonough, 1991; Vervoort and Patchett, 1996; Sylvester et al., 1997; Rudnick et al., 2000; Green et al., 2000; Campbell, 2003). Periodic addition to the depleted mantle reservoir of 'eclogitic' to 'pyroxenitic' crustal restites should be taken into account in such models.

5.4. Scale and frequency of delamination events

The main unconstrained parameter in this catalytic model is the scale and frequency of lower crustal delamination events. Zegers and van Keken (2001) suggested that the peaks in activity in the Pilbara at 3.47 and 3.45 Ga may reflect lower crustal delamination events (20 Ma interval). Van Kranendonk et al. (2002) documented an 11–37 Ma periodicity for the lower Pilbara Supergroup that they attributed to 8 plume events distributed over c. 300 Ma. Given that cratonization typically requires 200–300 Ma (e.g., Thurston, 1994; Leclair et al., 2001; cf. Caby, 2003), this suggests that something like 6–10 cycles may be appropriate for the entire cratonization process. Comparison with geochronological data from major plateau basalt provinces (e.g., Tejada et al., 2002; Prokoph et al., 2004) suggest a 25–35 Ma frequency for major pulses of melt delivery from mantle upwellings. It remains unclear whether the periodicity seen in cratons primarily reflects the mechanics of how melt segregates and is delivered from an ascending mantle column, the time-length-scales of major mantle mass instabilities (diapirs?), the time-length-scales of dense crustal restite delamination, or some harmonic of these rhythms.

5.5. Eclogitic catalysts in other mantle melting environments?

Recent petrogenetic models for many oceanic and continental plateau basalts involve a heterogeneous mantle source, where eclogitic material was picked up from depth (e.g., the 660 km disconinuity) by an ascending plume/diapir (Cordery et al., 1997; Yasuda et al., 1997; Takahashi et al., 1998; Yasuda and Fujii, 1998; Kerr et al., 2002; Révillon et al., 2002; Tejada et al., 2002). Is it possible that some oceanic and continental plateau basalts have developed eclogitic roots, which delaminated and mixed with the mantle beneath; so that the extra 'eclogitic' component needed to explain the huge volumes of melt seen in plateau basalts is derived from above, rather than being entrained from below? It may even be that the downward flux of crustal cumulate and restite plays a role in focussing, amplifying and anchoring the 'plume' (e.g., Shaw and Jackson, 1973).

The eclogite catalysis effect may not be restricted to anorogenic scenarios. There is evidence for extensive eclogitic delamination beneath the Cordillera (e.g., Ducea and Saleeby, 1998b; Ducea, 2002; Saleeby et al., 2003), and isotopic and trace element signatures of Pliocene-Quaternary lavas from this area might record mixing of delaminated eclogite with the mantle (see references in Saleeby et al., 2003). The high-SiO_2 'adakitic' glasses and metasomatic signatures observed in peridotite xenoliths from arc volcanos (Schiano et al., 1995; Kepezhinskas et al., 1996) might also result from melting delaminated lower crust (Ducea and Saleeby, 1998a), rather than melting of a subducted slab. It has also been proposed that delaminated Archaean eclogite was involved in the genesis of Jurassic high-magnesium andesites, dacites and adakites in China (Gao et al., 2004). I speculate that delamination-driven catalytic processes such as those outlined above might be an important, albeit unrecognized, magmagenetic process in Proterozoic to modern arcs, oceanic plateaux and oceanic ridges (Bédard, 1988; Arndt and Goldstein, 1989; Anderson, 1994; Saleeby et al., 2003).

6. A test

Can an objective test be devised for this family of hypotheses? An obvious 1st-order constraint is that melting of a mixed source composed of delaminated crustal restite and depleted harzburgitic mantle should generate a recognizable Archaean magma type. To this end, an equilibrium melting model was developed (e.g., Fig. 13) using a refertilized mantle source generated by mixing

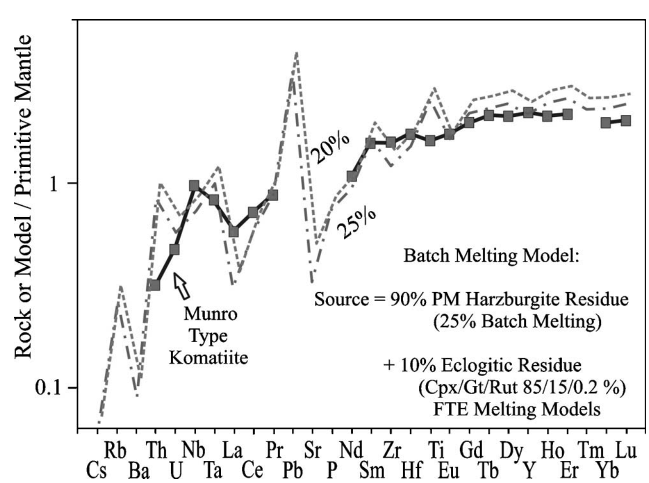

Fig. 13. Melts derived by 20–25% equilibrium melting of a refertilized mantle source with a harzburgitic residue. The source was generated by mixing 90% depleted harzburgite derived by c. 25% melting from a primitive mantle source (Bédard, 1999), and 10% of an eclogitic residue (rutile–eclogite from Fig. 8C) derived from 20% melting of the average Douglas Harbour metabasalt. The D values used in the model are given in Table 2. A harzburgite residue was assumed. Munro-type komatiite from (Campbell, 2003).

10% of the model eclogitic crustal restite produced from the Archaean metabasalt melting models outlined above (Fig. 8), with 90% of a harzburgitic mantle restite generated by extensive equilibrium melting of primitive mantle (Bédard, 1999). It was assumed that the refertilized source would melt sufficiently to completely exhaust the added phases, leaving behind a harzburgitic residue. Fig. 13 shows that the model melts generated by equilibrium melting of this refertilized source bear a strong resemblance to typical Munro-Type komatiites. If the results of this speculative model are correct, then this suggests that:

(1) Komatiites may not be large-degree melts initiated at great depths (garnet peridotite stability field) in the axes of large mantle plumes, but may be derived by refertilizing depleted shallow mantle with a delaminated crustal restite. Thus, the garnet trace element signatures of komatiites may be the fingerprints of crustal restite pollution from above, rather than recording equilibration with a garnet peridotite assemblage at great depth.
(2) The presence of water (hornblende, mica) in some of this delaminated material would facilitate komatiite generation by lowering peridotite solidus temperatures (cf. Parman and Grove, 2004).
(3) The different varieties of Archaean komatiite (Al-depleted, Al-undepleted) may reflect the proportion of clinopyroxene and garnet in the material added from above.
(4) The dominant 1-stage mantle melt derived from the plumes that initiate cratonization may be the common Archaean tholeiites (cf. Arndt et al., 1997), rather than komatiites. This implies that these plumes may not have been as hot as has been inferred on the basis of the komatiite phase equilibrium data.

7. Conclusions

The petrography and geochemistry of the TTG suite rocks from the NE Superior province (e.g., Bédard, 2003; Bédard et al., 2003; this paper Figs. 4–9), imply that tonalitic parental magmas formed by: (1) melting of a tholeiitic metabasite source, leaving behind a garnet-titanate-bearing pyroxenite/eclogite restite (high La/Yb, negative Nb–Ta–Ti anomalies); followed by (2) lower- to mid-crustal hornblende-dominated fractionation (e.g., increasing La/Yb, Sr/Y, decreasing HREE and Y) to generate trondhjemite. An arc environment is not required to explain the archetypal Archaean TTG geochemical signatures. Inferences from numerical and geophysical models (Figs. 2 and 3) suggest that Archaean arcs may not have operated efficiently, and that if they did, they could not have generated the volume of TTGs that dominate Archaean cratons. A plateau-melting model above a large Archaean 'plume' is favoured. In this model (Fig. 10), the base of basaltic plateaux melt due to ongoing mafic magmatism, yielding TTGs and complementary crustal restites composed of pyroxene + garnet + rutile. The high densities of pyroxene and garnet trigger negative gravitational instabilities. Mixing of eclogitic crustal restites with the depleted mantle would refertilize the mantle, allowing further melting (Figs. 11 and 12). Ascent of melt (heat) would trigger more crustal melting, and generate more eclogitic restite, which would then delaminate, mix, cause more mantle melting, and so on.... The eclogitic component would thus represent a catalyst for coupled crust–mantle differentiation in the Archaean. The catalytic model proposed here mitigates the mass balance problem inherent in the derivation of the TTG suite from a metabasite crustal source, since the huge volumes of unobserved restite required by such models would be destroyed bit-by-bit at shallow levels in the mantle. Refertilization of depleted upper mantle sources by delaminated crustal restites has the potential to generate melts with trace element signatures similar to those of typical Munro-Type komatiites (Fig. 13), a hypothesis that requires further testing. Thus, the model outlined above appears to account for the coexistence in a single tectonic environment (large plumes or major mantle overturns: Davies, 1995), of all major Archaean magma types. This reconciles the apparent dichotomy between the dominantly tholeiitic–komatiitic greenstone belts (plume source) and the TTG plutonic belts, for which arc affinities have been assumed hitherto. The model obviates the need for fortuitous slab windows to allow passage of plume-derived magmas through the subducting slab and greatly simplifies the geological history inferred for most Archaean cratons. If correct, the catalytic model outlined in this paper provides the missing genetic link that could relate the two fundamental building blocks of Archaean cratons. A complete rejection of mobilist scenarios is not implied, since progressive rigidification during cratonization implies a gradation towards more familiar uniformitarian magmatic and tectonic processes.

Acknowledgments

The ideas developed here benefitted from innumerable discussions with colleagues over the course of the past years. Reviews by Wouter Bleeker, Peter van Thienen, Nick Arndt, and others are gratefully acknowledged. This is Geological Survey of Canada paper # 2005438.

Associate editor: Martin A. Menzies

References

Abbott, D., Drury, R., Smith, W.H.F., 1994. A flat to steep transition in subduction style. *Geology* **22**, 937–940.

Abbott, D.H., Drury, R., Mooney, W.D., 1997. Continents as lithological icebergs: the importance of buoyant lithospheric roots. *Earth Planet. Sci. Lett.* **149**, 15–27.

Albarède, F., van der Hilst, R.D., 2002. Zoned mantle convection. *Phil. Trans. R. Soc. Lond. Ser. A. Math. Phys. Eng. Sci.* **360**, 2569–2592.

Anderson, D.L., 1994. The sublithospheric mantle as the source of continental flood basalts: the case against the continental lithosphere and plume head reservoirs. *Earth Planet. Sci. Lett.* **123**, 269–280.

Anhaeusser, C.R., Mason, R., Viljoen, M.J., Viljoen, R.P., 1969. Reappraisal of some aspects of Precambrian shield geology. *Bull. Geol. Soc. Am.* **80**, 2175–2200.

Annen, C., Sparks, R.S.J., 2002. Effects of repetitive emplacement of basaltic intrusions on thermal evolution and melt generation in the crust. *Earth Planet. Sci. Lett.* **203**, 937–955.

Arndt, N., 2003. Komatiites, kimberlites, and boninites. *J. Geophys. Res.* **108**. doi:10.1029/2002JB002157, art. no. 2293.

Arndt, N., 1999. Why was flood volcanism on submerged continental platforms so common in the Precambrian? *Prec. Res.* **97**, 155–164.

Arndt, N.T., Albarède, F., Nisbet, E.G., 1997. Mafic and ultramafic magmatism. In: de Wit, M.J., Ashwal, L.D. (Eds.), *Greenstone Belts*. Oxford Science Publ., Oxford, pp. 233–254.

Arndt, N.T., Goldstein, S.L., 1989. An open boundary between lower continental crust and mantle: its role in crust formation and crustal recycling. *Tectonophysics* **161**, 201–212.

Arndt, N.T., Lewin, É., Albarède, F., 2002. Strange Partners: formation and survical of continental crust and lithospheric mantle. In: Fowler, C.M.R., Ebinger, C.J., Hawkesworth, C.J. (Eds.), *The Early Earth: Physical, Chemical and Biological Development* vol. 199. Geol. Soc. London, Spec. Publ., Geol. Soc. London Publishing House, Brassmill Enterprises, Bath, UK, pp. 91–103.

Arth, J.G., Barker, F., Peterman, Z.E., Frideman, I., 1978. Geochemistry of the gabbro-diorite-tonalite-trondhjemite suite of southwest Finland and its implications for the origin of tonalitic and trondhjemitic magmas. *J. Petrol.* **19**, 289–316.

Arth, J.G., Hanson, G.N., 1972. Quartz diorites deived by partial melting of eclogite or amphibolite at mantle depths. *Contrib. Mineral. Petr.* **37**, 161–174.

Arth, J.G., Hanson, G.N., 1975. Geochemistry and origin of the early Precambrian crust of northeastern Minnesota. *Geochim. Cosmochim. Acta* **30**, 325–362.

Atherton, M.P., Petford, N., 1993. Generation of sodium-rich magmas from newly underplated basaltic crust. *Nature* **362**, 144–146.

Aulbach, S., Stachel, T., Viljoen, K.S., Brey, G.P., Harris, J.W., 2002. Eclogitic and websteritic diamond sources beneath the Limpopo Belt—is slab-melting the link? *Contrib. Mineral. Petr.* **143**, 56–70.

Ayer, J., Amelin, Y., Corfu, F., Kamo, S., Ketchum, J., Kwok, K., Trowell, N., 2002. Evolution of the southern Abitibi greenstone belt based on U-Pb geochronology: autochthonous volcanic construction followed by plutonism, regional deformation and sedimentation. *Prec. Res.* **115**, 63–95.

Ayres, L.D., Thurston, P.C., 1985. Archean supracrustal sequences in the Canadian Shield: an overview. In: Ayres, L.D., Thurston, P.C., Card, K.D., Weber, W. (Eds.), *Evolution of Archean Supracrustal Sequences, Special Paper 28*, Geol. Assoc. Can. Memorial University of Newfoundland, St. John's, pp. 343–380.

Bailey, R.C., 1999. Gravity-driven continental overflow and Archaean tectonics. *Nature* **398**, 413–415.

Baragar, W.R.A., McGlynn, J.C., 1976. Early Archaean basement in the Canadian Shield; a review of the evidence. *Geol. Surv. Can. Paper* **76–14**, 20.

Barker, F., Arth, J.G., 1976. Generation of trondhjemitic-tonalitic liquids and Archean bimodal trondhjemite-basalt suites. *Geology* **4**, 596–600.

Barrie, C.T., Ludden, J.N., Green, T.H., 1993. Geochemistry of volcanic rocks associated with Cu-Zn and Ni-Cu deposits in the Abitibi subprovince. *Econ. Geol.* **88**, 1314–1358.

Barth, M.G., Rudnick, R.L., Carlson, R.W., Horn, I., McDonough, W.F., 2002a. Re-Os and U-Pb geochronological constraints on the eclogite-tonalite connection in the Archean Man Shield, West Africa. *Prec. Res.* **118**, 267–283.

Barth, M.G., Foley, S.F., Horn, I., 2002b. Partial melting in Archean subduction zones: constraints from experimentally determined trace element partition coefficients between eclogitic minerals and tonalitic melts under upper mantle conditions. *Prec. Res.* **113**, 323–340.

Barth, M.G., Rudnick, R.L., Horn, I., McDonough, W.F., Spicuzza, M.J., Valley, J.W, Haggerty, S.E., 2002c. Geochemistry of xenolithic eclogites from West Africa, Part II: origins of the high MgO eclogites. *Geochim. Cosmochim. Acta* **66**, 4325–4345.

Barth, M.G., Rudnick, R.L., Horn, I., McDonough, W.F., Spicuzza, M.J., Valley, J.W., Haggerty, S.E., 2001. Geochemistry of xenolithic eclogites from West Africa, Part I: A link between low MgO eclogites and archean crust formation. *Geochim. Cosmochim. Acta* **65**, 1499–1527.

Beard, J.S., Lofgren, G.E., 1991. Dehydration melting and water-saturated melting of basaltic and andesitic greenstones and amphibolites at 1, 3, and 6.9 kb. *J. Petrol.* **32**, 365–401.

Bebout, G.E., Barton, M.D., 2002. Tectonic and metasomatic mixing in a high-T, subduction-zone melange—insights into the geochemical evolution of the slab-mantle interface. *Chem. Geol.* **187**, 79–106.

Bédard, J.H., 1988. Magma chamber dynamics and recycling of crustal cumulates by the mantle: evidence from the Bay of Islands ophiolite. *EOS Trans. Amer. Geophys. Union* **69**, 1476 (abstract).

Bédard, J.H., 1999. Petrogenesis of boninites from the Betts Cove Ophiolite, Newfoundland, Canada: Identification of subducted source components. *J. Petrol.* **40**, 1853–1889.

Bédard, J.H., 2003. Evidence for regional-scale, pluton-driven, high-grade metamorphism in the Archaean Minto Block, northern Superior Province, Canada. *J. Geol.* **111**, 183–205.

Bédard, J.H., 2005. Partitioning coefficients between olivine and silicate melts. *Lithos* **83**, 394–419.

Bédard, J.H., Berclaz, A., Hébert, R., Varfalvy, V., 2000. Syntexis and the genesis of the oceanic crust. In: Dilek, Y., Moores, E.M., Elthon, D., Nicolas, A. (Eds.), *Ophiolites and Oceanic Crust: New Insights from Field Studies and Ocean Drilling Program*, vol. 349. Geol. Soc. Am. Spec. Publ., Geological Society of America Special Paper, Boulder Colorado, USA, pp. 105–119.

Bédard, J.H., Brouillette, P., Madore, L., Berclaz, A., 2003. Archaean cratonization and deformation in the northern Superior Province, Canada: an evaluation of plate tectonic versus vertical tectonic models. *Prec. Res.* **127**, 61–87.

Bell, K., Blenkinsop, J., 1987. Archean depleted mantle: Evidence from Nd and Sr initial isotopic ratios of carbonatites. *Geochim. Cosmochim. Acta* **51**, 291–298.

Bickle, M.J., 1978. Heat loss from the Earth: a constraint on Archaean tectonics from the relation between geothermal gradients and the rate of plate production. *Earth Planet. Sci. Lett.* **40**, 301–315.

Bickle, M.J., 1986. Implications of melting for stabilization of the lithosphere and heat loss in the Archean. *Earth Planet. Sci. Lett.* **80**, 314–324.

Bickle, M.J., Bettenay, L.F., Chapman, H.J., Groves, D.I., McNaughton, N.J., Campbell, I.H., de Laeter, J.R., 1989. The age and origin of younger granitic plutons of the Shaw batholith in the Archaean Pilbara Block, Western Australia. *Contrib. Mineral. Petr.* **101**, 361–376.

Bickle, M.J., Nisbet, E.G., Martin, A., 1995. Archean greenstone belts are not oceanic crust. *J. Geol.* **102**, 121–138.

Bizimis, M., Salters, V.J.M., Bonatti, E., 2000. Trace and REE content of clinopyroxenes from supra-subduction zone peridotites. Implications for melting and enrichment processes in island arcs. *Chem. Geol.* **165**, 67–85.

Blake, T.S., Buick, R., Brown, S.J.A., Barley, M.E., 2004. Geochronology of a Late Archaean flood basalt province in the Pilbara Craton, Australia: constraints on basin evolution, volcanic and sedimentary accumulation, and continental drift rates. *Prec. Res.* **133**, 143–173.

Bleeker, W., 2002. Archaean tectonics: a review, with illustrations from the Slave craton. In: Fowler, C.M.R., Ebinger, C.J., Hawkesworth, C.J. (Eds.), *The Early Earth: Physical, Chemical and Biological Developments*, vol. 199. Geol. Soc. London Spec. Publ., Geol. Soc. London Publishing House, Brassmill Enterprises, Bath, UK, pp. 151–181.

Blundy, J.D., Wood, B.J., 1994. Prediction of crystal-melt partition coefficients from elastic moduli. *Nature* **372**, 452–454.

Bolhar, R., Woodhead, J.D., Hergt, J.M., 2003. Continental setting inferred for emplacement of the 2.9–2.7 Ga Belingwe Greenstone Belt, Zimbabwe. *Geology* **31**, 295–298.

Boudreau, A.E., 1999. PELE—a version of the MELTS software program for the PC platform. *Comp. Geosci.* **25**, 201–203.

Bouhallier, H., Chardon, D., Choukroune, P., 1995. Strain patterns in Archaean dome-and-basin structures: the Dharwar craton (Karnataka, south India). *Earth Planet. Sci. Lett.* **135**, 57–75.

Bowen, N.L., 1928. *The Evolution of the Igneous Rocks*. Princeton University Press, Princeton, NJ, 334p.

Boyd, F.R., 1998. The origin of cratonic peridotites: a major-element approach. *Int. Geol. Rev.* **40**, 755–764.

Brandon, A.D., Creaser, R.A., Chacko, T., 1996. Constraints on rates of granitic magma transport from epidote dissolution kinetics. *Science* **271**, 1845–1848.

Caby, R., 2003. Terrane assembly and geodynamic evolution of central-western Hoggar: a synthesis. *J. Afr. Earth Sci.* **37**, 133–159.

Cahill, J.T., Isacks, B.L., 1992. Seismicity and shape of the subducted Nazca Plate. *J. Geophys. Res.* **97**, 17503–17529.

Calmus, T., Aguillon-Robles, A., Maury, R.C., Bellon, H., Benoit, M., Cotten, J., Bourgois, J., Michaud, F., 2003. Spatial and temporal evolution of basalts and magnesian andesites ("bajaites") from Baja California, Mexico: the role of slab melts. *Lithos* **66**, 77–105.

Calvert, A.J., Ludden, J.N., 1999. Archean continental assembly in the southeastern Superior Province of Canada. *Tectonics* **18**, 412–429.

Campbell, I.H., 2003. Constraints on continental growth models from Nb/U ratios in the 3.5 Ga barberton and other Archaean basalt-komatiite suites. *Am. J. Sci.* **303**, 319–351.

Campbell, I.H., Griffiths, R.W., Hill, R.I., 1989. Melting in an Archaean mantle plume: heads it's basalts, tails it's komatiites. *Nature* **339**, 697–698.

Canil, D., 2004. Mildly incompatible elements in peridotites and the origins of mantle lithosphere. *Lithos* **77**, 375–393.

Card, K.D., 1990. A review of the Superior Province of the Canadian Shield, a product of Archean accretion. *Prec. Res.* **48**, 99–156.

Carlson, R.L., Hilde, T.W.C., Uyeda, S., 1983. The driving mechanism of plate tectonics: relation to age of the lithosphere at trenches. *Geophys. Res. Lett.* **10**, 297–300.

Carroll, M.R., Wyllie, P.J., 1989. Experimental phase relations in the system tonalite-peridotite-H_2O at 15 kb: implications for assimilation and differentiation processes near the crust-mantle boundary. *J. Petrol.* **30**, 1351–1382.

Castillo, P.R., Janney, P.E., Solidum, R.U., 1999. Petrology and geochemistry of Camiguin Island, southern Philippines: insights to the source of adakites and other lavas in a complex arc setting. *Contrib. Mineral. Petr.* **134**, 33–51.

Chardon, D., Choukroune, P., Jayananda, M., 1996. Strain patterns, decollement and incipient sagducted greenstone terrains in the Archaean Dharwar craton (south India). *J. Struct. Geol.* **18**, 991–1004.

Chardon, D., Choukroune, P., Jayananda, M., 1998. Sinking of the Dharwar Basin (south India): implications for Archaean tectonics. *Prec. Res.* **91**, 15–39.

Chardon, D., Peucat, J.J., Jayananda, M., Choukroune, P., Fanning, C.M., 2002. Archean granite-greenstone tectonics at Kolar (South India): Interplay of diapirism and bulk inhomogeneous contraction during juvenile magmatic accretion. *Tectonics* **21**, art. no. 1016.

Choukroune, P., Bouhallier, H., Arndt, N.T., 1995. Soft lithosphere during periods of Archaean crustal growth or crustal reworking. In: Coward, M.P., Ries, A.C. (Eds.), *Early Precambrian Processes*. vol. 95, Geol. Soc. London Spec. Publ., pp. 67–86.

Chown, E.H., Harrap, R., Moukhsil, A., 2002. The role of granitic intrusions in the evolution of the Abitibi belt, Canada. *Prec. Res.* **115**, 291–310.

Christensen, U.R., Hofmann, A.W., 1994. Segregation of subducted oceanic crust in the convecting mantle. *J. Geophys. Res.* **99**, 19867–19884.

Chung, S.L., Liu, D.Y., Ji, J.Q., Chu, M.F., Lee, H.Y., Wen, D.J., Lo, C.H., Lee, T.Y., Qian, Q., Zhang, Q., 2003. Adakites from continental collision zones: melting of thickened lower crust beneath southern Tibet. *Geology* **31**, 1021–1024.

Cloos, M., 1993. Lithospheric buoyancy and collisional orogenesis - Subduction of oceanic plateaus, continental margins, island arcs, spreading ridges, and seamounts. *Bull. Geol. Soc. Am.* **105**, 715–737.

Coffin, M.F., Eldholm, O., 1994. Large Igneous Provinces: crustal structure, dimensions, and external consequences. *Rev. Geophys.* **32**, 1–36.

Collins, W.J., 1993. Melting of Archaean sialic crust under high aH$_2$O conditions: genesis of 3300 Ma Na-rich granitoids in the Mount Edgar Batholith, Pilbara Block, Western-Australia. *Prec. Res.* **60**, 151–174.

Collins, W.J., Van Kranendonk, M.J., Teyssier, C., 1998. Partial convective overturn of Archaean crust in the east Pilbara Craton, Western Australia: driving mechanisms and tectonic implications. *J. Struct. Geol.* **20**, 1405–1424.

Condie, K.C., 1980. Origin and early development of the Earth's crust. *Prec. Res.* **11**, 183–197.

Condie, K.C., 1981. *Archean Greenstone Belts*. Elsevier, Amsterdam, 434p.

Condie, K.C., 1984. Archean geotherms and supracrustal assemblages. *Tectonophysics* **105**, 29–41.

Condie, K.C., 1986. Origin and early growth rate of continents. *Prec. Res.* **32**, 261–278.

Condie, K.C., 2005. TTGs and adakites: are they both slab melts? *Lithos* **80**, 33–44.

Conrey, R.M., Hooper, P.R., Larson, P.B., Chesley, J., Ruiz, J., 2001. Trace element and isotopic evidence for two types of crustal melting beneath a High Cascade volcanic center, Mt. Jefferson, Oregon. *Contrib. Mineral. Petr.* **141**, 710–732.

Cordery, M.J., Davies, G.F., Campbell, I.H., 1997. Genesis of flood basalts from eclogite-bearing mantle plumes. *J. Geophys. Res.* **102**, 20179–20197.

Daigneault, R., Mueller, W.U., Chown, E.H., 2002. Oblique Archean subduction: accretion and exhumation of an oceanic arc during dextral transpression, Southern Volcanic Zone, Abitibi Subprovince Canada. *Prec. Res.* **115**, 261–290.

Davidson, D.M.J., 1980. Emplacement and deformation of the Archean Saganaga batholith, Vermilion district, northeastern Minnesota. *Tectonophysics* **66**, 179–195.

Davies, G.F., 1979. Thickness and thermal history of continental crust and root zones. *Earth Planet. Sci. Lett.* **44**, 231–238.

Davies, G.F., 1992. On the emergence of plate tectonics. *Geology* **20**, 963–966.

Davies, G.F., 1993. Conjectures on the thermal and tectonic evolution of the Earth. *Lithos* **30**, 281–289.

Davies, G.F., 1995. Punctuated tectonic evolution of the Earth. *Earth Planet. Sci. Lett.* **136**, 363–379.

Davis, D.W., Edwards, G.R., 1986. Crustal evolution of Archean rocks in the Kakagi Lake area, Wabigoon subprovince, northwest Ontario. *Can. J. Earth Sci.* **23**, 182–192.

Davis, D.W., Pezzutto, F., Ojakangas, R.W., 1990. The age and provenance of metasedimentary rocks in the Quetico subprovince, Ontario, from single zircon analyses: implications for Archean sedimentation and tectonics in the Superior Province. *Earth Planet. Sci. Lett.* **99**, 195–205.

Davis, W.J., Jones, A.G., Bleeker, W., Grutter, H., 2003. Lithosphere development in the Slave craton: a linked crustal and mantle perspective. *Lithos* **71**, 575–589.

Davis, W.J., Sutcliffe, R.H., Trowell, N.F., 1988. Geochronological constraint son the tectonic evolution of a Late Archaean greenstone belt, Wabigoon subprovince, northwest Ontario, Canada. *Prec. Res.* **39**, 171–191.

De Smet, J., Van den Berg, A.P., Vlaar, N.J., 2000. Early formation and long-term stability of continents resulting from decompression melting in a convecting mantle. *Tectonophysics* **322**, 19–33.

Defant, M.J., Kepezhinskas, P., 2001. Evidence suggests slab melting in arc magmas. *EOS Trans. Am. Geophys. Union* **82**, 65–69.

Desrochers, J.-P., Hubert, C., Ludden, J.N., Pilote, P., 1993. Accretion of Archean oceanic plateau fragments in the Abitibi greenstone belts, Canada. *Geology* **21**, 451–454.

de Wit, M.J., 1998. On Archean granites, greenstones, cratons and tectonics: does the evidence demand a verdict? *Prec. Res.* **91**, 181–226.

de Wit, M.J., Roering, C., Hart, R.J., Armstrong, R.A., Deronde, C.E.J., Green, R.W.E., Tredoux, M., Peberdy, E., Hart, R.A., 1992. Formation of an Archaean Continent. *Nature* **357**, 553–562.

Dick, H.J.B., Fisher, R.L., Bryan, W.B., 1984. Mineralogic variability of the uppermost mantle along mid-ocean ridges. *Earth Planet. Sci. Lett.* **69**, 88–106.

Dimroth, R., Imreh, L., Rocheleau, M., Goulet, N., 1982. Evolution of the south-central part of the Archean Abitibi belt. Part I: stratigraphy and paleogeographical model. In: Baer, A.J. (Ed.), *Basins and Geosynclines of the Canadian Shield*, *Geol. Surv. Can. Paper*, vol. 19, pp. 1729–1758.

Dirks, P.H.G.M., Jelsma, H.A., 1998a. Horizontal accretion and stabilization of the Archean Zimbabwe craton. *Geology* **26**, 11–14.

Dirks, P.H.G.M., Jelsma, H.A., 1998b. Horizontal accretion and stabilization of the Archean Zimbabwe Craton: Reply. *Geology* **26**, 1147–1150.

Dirks, P.H.G.M., Jelsma, H.A., Hofmann, A., 2002. Thrust-related accretion of an Archaean greenstone belt in the Midlands of Zimbabwe. *J. Struct. Geol.* **24**, 1707–1727.

Drummond, M.S., Defant, M.J., 1990. A model for trondhjemite–tonalite–dacite genesis and crustal growth via slab melting—Archean to modern comparisons. *J. Geophys. Res.* **95**, 21503–21521.

Drummond, M.S., Defant, M.J., Kepezhinskas, P.K., 1996. Petrogenesis of slab-derived trondhjemite-tonalite-dacite/adakite magmas. *Trans. R. Soc. Edinburgh—Earth Sci.* **87**, 205–215.

Drury, S.A., Harris, N.B., Holt, R.W., Reeves-Smith, G.J., Wightman, R.T., 1984. Precambrian tectonics and crustal evolution on South India. *J. Geol.* **92**, 3–20.

Ducea, M.N., 2002. Constraints on the bulk composition and root foundering rates of continental arcs: a California arc perspective. *J. Geophys. Res.* **107**. doi:10.1029/2001JB000643, art. no. 2304.

Ducea, M., Saleeby, J., 1998a. A case for delamination of the deep batholithic crust beneath the Sierra Nevada, California. *Int. Geol. Rev.* **40**, 78–93.

Ducea, M., Saleeby, J., 1998b. Crustal recycling beneath continental arcs: silica-rich glass inclusions in ultramafic xenoliths from the Sierra Nevada, California. *Earth Planet. Sci. Lett.* **156**, 101–116.

Dumitru, T.A., Gans, P.B., Foster, D.A., Miller, E.L., 1991. Refrigeration of the western Cordilleran lithosphere during Laramide shallow-angle subduction. *Geology* **19**, 1145–1148.

Durrheim, R., Mooney, W.D., 1994. Evolution of the Precambrian lithosphere: seismological and geochemical constraints. *J. Geophys. Res.* **99**, 15359–15374.

du Vignaux, N.M., Fleitout, L., 2001. Stretching and mixing of viscous blobs in Earth's mantle. *J. Geophys. Res.* **106**, 30893–30908.

Dzwinel, W., Yuen, D.A., 2001. Mixing driven by Rayleigh-Taylor instability in the mesoscale modeled with dissipative particle dynamics. *Int. J. Mod. Phys. C* **12**, 91–118.

Farnetani, C.G., Legras, B., Tackley, P.J., 2002. Mixing and deformations in mantle plumes. *Earth Planet. Sci. Lett.* **196**, 1–15.

Feng, R., Kerrich, R., 1992. Geochemical evolution of Granitoids from the Archean Abitibi Southern Volcanic Zone and the Pontiac Subprovince, Superior Province, Canada—implications for tectonic history and source regions. *Chem. Geol.* **98**, 23–70.

Ferrachat, S., Ricard, Y., 1998. Regular vs. chaotic mantle mixing. *Earth Planet. Sci. Lett.* **155**, 75–86.

Foley, S.F., Barth, M.G., Jenner, G.A., 2000. Rutile/melt partition coefficients for trace elements and an assessment of the influence of rutile on the trace element characteristics of subduction zone magmatism. *Geochim. Cosmochim. Acta* **64**, 933–938.

Foley, S.F., Tiepolo, M., Vannucci, R., 2002. Growth of early continental crust controlled by melting of amphibolite in subduction zones. *Nature* **417**, 837–840.

Fountain, D.M. 1989. Growth and modification of lower continental crust in extended terrains: The role of extension and magmatic underplating. In: Mereu, R.F., Mueller, S. Fountain, D.M. (Eds.), *Properties and Processes of Earth's Lower Crust*, *Am. Geophys. Union Monogr.*, 51, IUGG Volume 6. American Geophysical Union, Washington, DC, pp. 287–299.

Fyfe, W.S., 1978. The evolution of the Earth's crust: modern plate tectonics to ancient hot spot tectonics? *Chem. Geol.* **23**, 89–114.

Gao, S., Luo, T.C., Zhang, B.R., Zhang, H.F., Han, Y.W., Zhao, Z.D., Hu, Y.K., 1998b. Chemical composition of the continental crust as revealed by studies in East China. *Geochim. Cosmochim. Acta* **62**, 1959–1975.

Gao, S., Rudnick, R.L., Yuan, H.L., Liu, X.M., Liu, Y.S., Xu, W.L., Ling, W.L., Ayers, J., Wang, X.C., Wang, Q.H., 2004. Recycling lower continental crust in the North China craton. *Nature* **432**, 892–897.

Gao, S., Zhang, B.R., Jin, Z.M., Kern, H., Luo, T.C., Zhao, Z.D., 1998a. How mafic is the lower continental crust. *Earth Planet. Sci. Lett.* **161**, 101–117.

Gariépy, C., Allègre, C.J., 1985. The lead isotope geochemistry and geochronology of late-kinematic intrusives from the Abitibi greenstone belt, and the implications for late Archaean crustal evolution. *Geochim. Cosmochim. Acta* **49**, 2371–2383.

Ghiorso, M.S., Hirschmann, M.M., Reiners, P.W., Kress, V.C., 2002. The pMELTS: A revision of MELTS for improved calculation of phase relations and major element partitioning related to partial melting of the mantle to 3 GPa. *Geochem. Geophys. Geosys.*, 3U1–U36.

Glazner, A.F., 1994. Foundering of mafic plutons and density stratification of continental crust. *Geology* **22**, 435–438.

Glikson, A.Y., 1972. Early Precambrian evidence of a primitive ocean crust and island nuclei of sodic granite. *Bull. Geol. Soc. Am.* **83**, 3323–3344.

Goodwin, A.M., 1981. Archaean plates and greenstone belts. In: Kröner, A. (Ed.), *Precambrian Plate Tectonics*. Elsevier, Amsterdam, pp. 105–135.

Goodwin, A.M., 1996. *Principles of Precambrian Geology*. Academic Press, London, 327p.

Green, D.H., Falloon, T.J., 1998. Pyrolite: a Ringwood concept and its current expression. In: Jackson, I. (Ed.), *The Earth's Mantle: Composition, Structure and Evolution*. Cambridge University Press, Cambridge, UK, pp. 311–378.

Green, M.G., Sylvester, P.J., Buick, R., 2000. Growth and recycling of early Archaean continental crust: geochemical evidence from the Coonterunah and Warrawoona Groups, Pilbara Craton, Australia. *Tectonophysics* **322**, 69–88.

Green, T.H., Pearson, N.J., 1986. Ti-rich accessory phase saturation in hydrous mafic-felsic compositions at high P, T. *Chem. Geol.* **54**, 185–201.

Griffin, W.L., O'Reilly, S.Y., Abe, N., Aulbach, S., Davies, R.M., Pearson, N.J., Doyle, B.J., Kivi, K., 2003. The origin and evolution of Archean lithospheric mantle. *Prec. Res.* **127**, 19–41.

Grove, T.L., Parman, S.W., 2004. Thermal evolution of the Earth as recorded by komatiites. *Earth Planet. Sci. Lett.* **219**, 173–187.

Gutscher, M.A., Peacock, S.M., 2003. Thermal models of flat subduction and the rupture zone of great subduction earthquakes. *J. Geophys. Res.* **108**. doi:10.1029/2001JB000787, art. 2009.

Hargraves, R.B., 1986. Faster spreading or greater ridge length in the Archean? *Geology* **14**, 750–752.

Hamilton, W.B., 1998. Archean tectonics and magmatism. *Int. Geol. Rev.* **40**, 1–39.

Harry, D.L., Green, N.L., 1999. Slab dehydration and basalt petrogenesis in subduction systems involving very young oceanic lithosphere. *Chem. Geol.* **160**, 309–333.

Helmstaedt, H.H., Doig, R., 1975. Eclogite nodules from kimberlite pipes of the Colorado Plateau—samples of subducted, Franciscan-type oceanic lithosphere. *Phys. Chem. Earth* **9**, 95–112.

Helmstaedt, H.H., Schulze, D.J., 1986. Southern African kimberlites and their mantle sample: implications for Archean tectonics and lithosphere evolution. In: Ross, J. (Ed.), *Kimberlites and Related Rocks*, *Spec. Publ. Geol. Soc. Australia*, vol. 14. Blackwell Publ., Carleton, pp. 358–368.

Herzberg, C., 1999. Phase equilibrium constraints on the formation of cratonic mantle. In: Fei, Y., Bertka, C.M., Mysen, B.O. (Eds.), *Mantle Petrology, Field Observations and High Pressure Experimentation: A Tribute to Francis R. (Joe) Boyd*, *Geoch. Soc. Spec. Publ.*, vol. 6. The Geochemical Society, Washington, DC, pp. 241–257.

Herzberg, C., 2004. Geodynamic information in peridotite petrology. *J. Petrol.* **45**, 2507–2530.

Herzberg, C.T., Fyfe, W.S., Carr, M.J., 1983. Density constraints on the formation of the continental Moho and crust. *Contrib. Mineral. Petrol.* **84**, 1–5.

Hickman, A.H., 1983. Geology of the Pilbara block and its environs. *Geol. Surv. West Australia Bull.* **127**, 268p.

Hickman, A.H., 1984. Archaean diapirism in the Pilbara Block, Western Australia. In: Kröner, A., Greiling, R. (Eds.), *Precambrian Tectonics Illustrated*. E. Schweizerbarts'che Verlagsbuchhandlung, Stuttgart, pp. 113–127.

Hickman, A.H., 2004. Two contrasting granite-greenstone terranes in the Pilbara Craton, Australia: evidence for vertical and horizontal tectonic regimes prior to 2900 Ma. *Prec. Res.* **131**, 153–172.

Hill, R.H., Campbell, I.H., Compston, W., 1989. Age and origin of granitic rocks in the Kalgoorlie-Norseman region of Western Australia: Implications for the origin of Archaean crust. *Geochim. Cosmochim. Acta* **53**, 1259–1275.

Hirschmann, M.M., Kogiso, T., Baker, M.B., Stolper, E.M., 2003. Alkalic magmas generated by partial melting of garnet pyroxenite. *Geology* **31**, 481–484.

Hoffman, P.F., Ranalli, G., 1988. Archean oceanic flake tectonics. *Geophys. Res. Lett.* **15**, 1077–1080.

Hofmann, A.W., White, W.M., 1982. Mantle plumes from ancient oceanic crust. *Earth Planet. Sci. Lett.* **57**, 421–436.

Horng, W.S., Hess, P.C., 2000. Partition coefficients of Nb and Ta between rutile and anhydrous haplogranite melts. *Contrib. Mineral. Petr.* **138**, 176–185.

Howell, D.G., 1989. How the growth and freeboard of continents may relate to geometric and kinematic parameters of mid-ocean spreading ridges. In: Ashwal, L.D. (Ed.), *Growth of the Continental Crust*, *Tectonophysics*, **161**, 343–349.

Huang, Y.M., Van Calsteren, P., Hawkesworth, C.J., 1995. The evolution of the lithosphere in southern Africa: A perspective on the basic granulite xenoliths from kimberlites in South Africa. *Geochim. Cosmochim. Acta* **59**, 4905–4920.

Huppert, H.E., Sparks, R.S.J., 1988. The generation of granitic magmas by intrusion of basalt into continental crust. *J. Petrol.* **29**, 599–624.

Ireland, T.R., Rudnick, R.L., Spetsius, Z., 1994. Trace elements in diamond inclusions from eclogites reveal link to Archaean granites. *Earth Planet. Sci. Lett.* **128**, 199–213.

Jacob, D.E., 2004. Nature and origin of eclogite xenoliths from kimberlites. *Lithos* **77**, 295–316.

Jacob, D.E., Foley, S.F., 1999. Evidence for Archean ocean crust with low high field strength element signature from diamondiferous eclogite xenoliths. *Lithos* **48**, 317–336.

Jacob, D., Jagoutz, E., Lowry, D., Mattey, D., Kudrjavtseva, G., 1994. Diamondiferous eclogites from Siberia: Remnants of Archean oceanic crust. *Geochim. Cosmochim. Acta* **58**, 5191–5207.

Jahn, B.M., Glikson, A.Y., Peucat, J.J., Hickman, A.H., 1981. REE geochemistry and isotopic data of Archean silicic volcanics and granitoids from the Pilbara Block, Western Australia: implications for early crustal evolution. *Geochim. Cosmochim. Acta* **45**, 1633–1652.

Jakobsson, S.P., 1972. Chemistry and distribution pattern of Recent basaltic rocks in Iceland. *Lithos* **5**, 345–364.

Jang, Y.D., Naslund, H.R., 2003. Major and trace element variation in ilmenite in the Skaergaard Intrusion: petrologic implications. *Chem. Geol.* **193**, 109–125.

Jellinek, A.M., Kerr, R.C., Griffiths, R.W., 1999. Mixing and compositional stratification produced by natural convection 1. Experiments and their application to Earth's core and mantle. *J. Geophys. Res.* **104**, 7183–7201.

Ji, S.C., Wang, Q., Xia, B., Marcotte, D., 2004. Mechanical properties of multiphase materials and rocks: a phenomenological approach using generalized means. *J. Struct. Geol.* **26**, 1377–1390.

Johnson, K.T.M., Dick, H.J.B., 1992. Open system melting and temporal and spatial variation of peridotite and basalt at the Atlantis-II Fracture Zone. *J. Geophys. Res.* **97**, 9219–9241.

Jordan, T.H., 1988. Structure and formation of the continental tectosphere. *J. Petrol. Special Lithosphere Issue*, 11–37.

Jull, M., Kelemen, P.B., 2001. On the conditions for lower crustal convective instability. *J. Geophys. Res.* **106**, 6423–6446.

Kamber, B.S., Ewart, A., Collerson, K.D., Bruce, M.C., McDonald, G.D., 2002. Fluid-mobile trace element constraints on the role of slab melting and implications for Archaean crustal growth models. *Contrib. Mineral. Petr.* **144**, 38–56.

Kay, R.W., 1978. Aleutian magnesian andesites: melts from subducted Pacific oceanic crust. *J. Volc. Geoth. Res.* **4**, 117–132.

Kay, R.W., Kay, S.M., 1991. Creation and destruction of lower continental crust. *Geol. Rundsch.* **80**, 259–278.

Kelemen, P.B., Hanghoj, K., Greene, A.R., 2004a. One view of the geochemistry of subduction-related magmatic arcs, with an emphasis on primitive andesite and lower crust. In: Rudnick, R.L. (Ed.), *The Crust*, *Treatise on Geochemistry*, vol. 3. Elsevier, Pergamon, San Diego, pp. 593–659.

Kelemen, P.B., Hart, S.R., Bernstein, S., 1998. Silica enrichment in the continental upper mantle via melt/rock reaction. *Earth Planet. Sci. Lett.* **164**, 387–406.

Kelemen, P.B., Rilling, J.L., Parmentier, E.M., Mehl, L., Hacker, B.R., 2004b. Thermal structure due to solid-state flow in the mantle wedge beneath arcs. In: Eiler, J. (Ed.), *The Subduction Zone Factory, Am. Geophys. Union Geophys. Monog.*, vol. 138. Elsevier, Pergamon, San Diego, pp. 293–311.

Kepezhinskas, P., Defant, M.J., Drummond, M.S., 1996. Progressive enrichment of island arc mantle by melt-peridotite interaction inferred from Kamchatka xenoliths. *Geochim. Cosmochim. Acta* **60**, 1217–1229.

Kepezhinskas, P., McDermott, F., Defant, M.J., Hochstaedter, A., Drummond, M.S., Hawkesworth, C.J., Koloskov, A., Maury, R.C., Bellon, H., 1997. Trace element and Sr-Nd-Pb isotopic constraints on a three-component model of Kamchatka arc petrogenesis. *Geochim. Cosmochim. Acta* **61**, 577–600.

Kerr, A.C., Tarney, J., Kempton, P.D., Spadea, P., Nivia, A., Marriner, G.F., Duncan, R.A., 2002. Pervasive mantle plume head heterogeneity: evidence from the late Cretaceous Caribbean-Colombian oceanic plateau. *J. Geophys. Res.* **107**. doi:10.1029/2001JB000790, art. no. 2140.

Kerr, A.C., Tarney, J., Marriner, G.F., Nivia, A., Saunders, A.D., 1997. The Caribbean-Colombian Cretaceous Igneous Province: The internal anatomy of an oceanic plateau. In: Mahoney, J., Coffin, M. (Eds.), *Large Igneous Provinces, Continental, Oceanic and Planetary Flood Volcanism, Am. Geophys. Union Geophys. Monog.*, vol. 100. American Geophysical Union, Washington, DC, pp. 123–144.

Kerr, A.C., Tarney, J., Nivia, A., Marriner, G.F., Saunders, A.D., 1998. The internal structure of oceanic plateaus: inferences from obducted Cretaceous terranes in western Colombia and the Caribbean. *Tectonophysics* **292**, 173–188.

Kerrich, R., Polat, A., Wyman, D., Hollings, P., 1999. Trace element systematics of Mg-, to Fe-tholeiitic basalt suites of the Superior Province: implications for Archean mantle reservoirs and greenstone belt genesis. *Lithos* **46**, 163–187.

Kerrich, R., Wyman, D., Fan, J., Bleeker, W., 1998. Boninite series: low Ti-tholeiite associations from the 2.7 Ga Abitibi greenstone belt. *Earth Planet. Sci. Lett.* **164**, 303–316.

Kerrich, R., Xie, Q.L., 2002. Compositional recycling structure of an Archean super-plume: Nb-Th-U-LREE systematics of Archean komatiites and basalts revisited. *Contrib. Mineral. Petr.* **142**, 476–484.

Ketchum, J.W.F., Bleeker, W., Stern, R.A., 2004. Evolution of an Archean basement complex and its autochtonous cover, southern Slave Province, Canada. *Prec. Res.* **135**, 149–176.

Kimura, G., Ludden, J.N., Desrochers, J.P., Hori, R., 1993. A model of ocean-crust accretion for the Superior Province, Canada. *Lithos* **30**, 337–355.

Kincaid, C., Sacks, I.S., 1997. Thermal and dynamical evolution of the upper mantle in subduction zones. *J. Geophys. Res.* **102**, 12295–12315.

Kleinhanns, I.C., Kramers, J.D., Kamber, B.S., 2003. Importance of water for Archaean granitoid petrology: a comparative study of TTG and potassic granitoids from Barberton Mountain Land, South Africa. *Contrib. Mineral. Petr.* **145**, 377–389.

Klemme, S., Blundy, J.D., Wood, B.J., 2002. Experimental constraints on major and trace element partitioning during partial melting of eclogite. *Geochim. Cosmochim. Acta* **66**, 3109–3123.

Kogiso, T., Hirschmann, M.M., Frost, D.J., 2003. High-pressure partial melting of garnet pyroxenite: possible mafic lithologies in the source of ocean island basalts. *Earth Planet. Sci. Lett.* **216**, 603–617.

Kogiso, T., Hirschmann, M.M., Pertermann, M., 2004. High-pressure partial melting of mafic lithologies in the mantle. *J. Petrol.* **45**, 2407–2422.

Kouchi, A., Sunagawa, I., 1985. A model for mixing basaltic and dacitic magmas as deduced from experimental data. *Contrib. Mineral. Petr.* **89**, 17–23.

Koyaguchi, T., Kaneko, K., 1999. A two-stage thermal evolution model of magmas in continental crust. *J. Petrol.* **40**, 241–254.

Kröner, A., 1985. Evolution of the Archaean continental crust. *Ann. Review Earth Planet. Sci.* **13**, 49–74.

Kröner, A., 1991. Tectonic evolution in Archaean and Proterozoic. *Tectonophysics* **187**, 393–410.

Kumagai, I., 2002. On the anatomy of mantle plumes: effect of the viscosity ratio on entrainment and stirring. *Earth Planet. Sci. Lett.* **198**, 211–224.

Kusky, T.M., 1998. Tectonic setting and terrane accretion of the Archean Zimbabwe craton. *Geology* **26**, 163–166.

Kusky, T.M., Kidd, W.S.F., 1992. Remnants of an Archean Oceanic Plateau, Belingwe Greenstone Belt, Zimbabwe. *Geology* **20**, 43–46.

Kusky, T.M., Polat, A., 1999. Growth of granite-greenstone terranes at convergent margins, and stabilization of Archean cratons. *Tectonophysics* **305**, 43–73.

Laflèche, M.R., Dupuy, C., Dostal, J., 1992. Tholeiitic volcanic rocks of the late Archean Blake River Group, southern Abitibi greenstone belt: Origin and geodynamic implications. *Can. J. Earth Sci.* **29**, 1448–1458.

Lambert, R.St.-J., 1976. Archaean thermal regimes, crustal and upper mantle temperatures, and a progressive evolutionary model for the Earth. In: Windley, B.F. (Ed.), *The Early History of the Earth*. J.Wiley, London, pp. 363–373.

Lambert, R.St-J., 1981. Earth tectonics and thermal history: review and a hot spot model for the Archaean. In: Kröner, A. (Ed.), *Precambrian Plate Tectonics*. Elsevier, Amsterdam, pp. 453–467.

Leclair, A., Berclaz, A., David, J., Percival, J.A., 2001. Regional geological setting of Archean rocks in the northeastern Superior Province. *Geol. Assoc. Can. /Mineral. Assoc. Can. Abstracts with Program* **26**, 84 (abstract).

Lenardic, A., Moresi, L.N., Muhlhaus, H., 2003. Longevity and stability of cratonic lithosphere: insights from numerical simulations of coupled mantle convection and continental tectonics. *J. Geophys. Res.* **108**. doi:10.1029/2002JB001859, art. 2303.

Lesher, C.M., Goodwin, A.M., Campbell, I.H., Gorton, M.P., 1986. Trace element geochemistry of ore-associated and barren, felsic metavolcanic rocks in the Superior province, Canada. *Can. J. Earth Sci.* **23**, 222–237.

Liu, T.-C., Presnall, D.C., 1990. Liquidus phase relationships on the join anorthite-forsterite-quartz at 20 kbar with applications to basalt petrogenesis and igneous spphirine. *Contrib. Mineral. Petrol.* **104**, 735–742.

Lowe, D.R., 1982. Comparative sedimentology of the principal volcanic sequences of Archean greenstone belts in South Africa, Western Australia and Canada: implications for crustal evolution. *Prec. Res.* **17**, 1–29.

Lowe, D.R., 1999. Geologic evolution of the Barberton greenstone belt and vicinity. In: Lowe, D.R., Byerly, G.R. (Eds.), *Geologic Evolution of the Barberton Greenstone Belt, South Africa, Geol. Soc. Am. Spec. Paper*, vol. 329, pp. 87–312.

Luais, B., Hawkesworth, C.J., 1994. The generation of continental crust: an integrated study of crust-forming processes in the Archaean of Zimbabwe. *J. Petrol.* **35**, 43–93.

Maaløe, S., 1982. Petrogenesis of Archaean tonalites. *Geol. Rundsch.* **71**, 328–346.

Maaløe, S., 1985. *Principles of Igneous Petrology*. Springer-Verlag, Berlin, 364p.

Macdonald, R., Hawkesworth, C.J., Heath, E., 2000. The Lesser Antilles Volcanic chain: a study in arc magmatism. *Earth Sci. Rev.* **49**, 1–76.

Macgregor, A.M., 1951. Some milestones in the Precambrian of Southern Africa. *Proc. Geol. Soc. South Africa* **54**, 27–71.

MacKenzie, J.M., Canil, D., 1999. Composition and thermal evolution of cratonic mantle beneath the central Archean Slave Province, NWT, Canada. *Contrib. Mineral. Petrol.* **134**, 313–324.

Madore, L., Bandyayera, D., Bédard, J.H., Brouillette, P., Sharma, K.N.M., Beaumier, M., David, J., 1999. Géologie de la région du Lac Peters (SNRC 24M). *Minist. Ress. Nat. Québec. Rapp. Géol.* **RG 99-07**, 41.

Madore, L., Larbi, Y., 2000. Géologie de la région de la Rivière Arnaud (SNRC 25D) et des régions littorales adjacentes (SNRC 25C, 25E et 25F). *Minist. Ress. Nat. Québec. Rapp. Géol.* **RG 2000-05**, 37p.

Madore, L., Larbi, Y., Sharma, K.M.M., Labbé, J.-Y., Lacoste, P., David, J., Brousseau, K., Hocq, M., 2001. Géologie de la région du lac Klotz (SNRC 35A) et du cratère du Nouveau-Québec (1/2 sud de SNRC 35H). *Minist. Ress. Nat. Québec. Rapp. Géol.* **RG 2001-09**, 44.

Manga, M., 1996. Mixing of hetereogeneities in the mantle: effect of viscosity differences. *Geophys. Res. Lett.* **23**, 403–406.

Mann, P., Taira, A., 2004. Global tectonic significance of the Solomon Islands and Ontong Java Plateau convergent zone. *Tectonophysics* **389**, 137–190.

Marshall, L.A., Sparks, R.S.J., 1984. Origin of some mixed-magma and net-veined ring intrusions. *J. Geol. Soc. Lond.* **141**, 171–182.

Martin, H., 1986. Effect of steeper Archean geothermal gradient on geochemistry of subduction-zone magmas. *Geology* **14**, 753–756.

Martin, H., 1987. Petrogenesis of Archean trondhjemites, tonalites, and granodiorites from eastern Finland: major and trace element geochemistry. *J. Petrol.* **28**, 921–953.

Martin, H., 1993. The mechanisms of petrogenesis of the Archean continental crust—comparison with modern processes. *Lithos* **30**, 373–388.

Martin, H., 1999. Adakitic magmas: modern analogues of Archaean granitoids. *Lithos* **46**, 411–429.

Martin, H., Moyen, J.F., 2002. Secular changes in tonalite-trondhjemite-granodiorite composition as markers of the progressive cooling of Earth. *Geology* **30**, 319–322.

Martin, H., Smithies, R.H., Rapp, R., Moyen, J.F., Champion, D., 2005. An overview of adakite, tonalite-trondhjemite-granodiorite (TTG), and sanukitoid: relationships and some implications for crustal evolution. *Lithos* **79**, 1–24.

McCall, G.J.H., 2003. A critique of the analogy between Archaean and Phanerozoic tectonics based on regional mapping of the Mesozoic-Cenozoic plate convergent zone in the Makran, Iran. *Prec. Res.* **127**, 5–17.

McCulloch, M.T., Wasserburg, G.J., 1978. Sm-Nd and Rb-Sr chronology of continental crust formation. *Science* **200**, 1003–1011.

McDonough, W.F., 1991. Partial melting of subducted oceanic crust and isolation of its residual eclogitic lithology. *Phil. Trans. R. Soc. Lond.* **A335**, 407–418.

Mège, D., Chardon, D., Hansen, V.L., 2000. Rayleigh-Taylor instability-driven plume tectonics and the rheology of the Archean, venusian and Martian crusts. *Lunar Planet. Sci.* **XXXI**, CD-ROM.

Miyashiro, A., 1974. Volcanic rock series in island arcs and active continental margins. *Am. J. Sci.* **274**, 321–355.

Moresi, L.N., Solomatov, V., 1998. Mantle convection with a brittle lithosphere: thoughts on the global tectonic styles of the Earth and Venus. *Geophys. J. Int.* **133**, 669–682.

Morgan, P., Phillips, R.J., 1984. Hot spot heat transfer: its application to Venus and Earth. *J. Geophys. Res.* **88**, 8305–8317.

Moser, D.E., Flowers, R.M., Hart, R.J., 2001. Birth of the Kaapvaal tectosphere 3.08 billion years ago. *Science* **291**, 465–468.

Moser, D.E., Heaman, L.M., Krogh, T.E., Hanes, J.A., 1996. Intracrustal extension of an Archean orogen revealed using single-grain U-Pb zircon geochronology. *Tectonics* **15**, 1093–1109.

Moyen, J.F., Martin, H., Jayananda, M., 2001. Multi-element geochemical modelling of crust-mantle interactions during late-Archaean crustal growth: the Closepet granite (South India). *Prec. Res.* **112**, 87–105.

Moyen, J.-F., Stevens, G., 2005. Experimental constraints on TTG petrogenesis: implications for Archaean geodynamics. In: Benn, K., Condie, K., Mareschal, J.C., (Eds.), *Archaean geodynamics and environments', AGU Monograph 164*. American Geophysical Union, Washington, DC (Chapter 10) (in press).

Muir, R.J., Weaver, S.D., Bradshaw, J.D., Eby, G.N., Evans, J.A., 1995. The Cretaceous Separation Point batholith, New Zealand: granitoid magmas formed by melting of mafic lithosphere. *J. Geol. Soc. Lond.* **152**, 689–701.

Neal, C.R., Mahoney, J.J., Kroenke, L.W., Duncan, R.A., Petterson, M.G., 1997. The Ontong Java Plateau. In: Mahoney, J.J., Coffin, M.F. (Eds.), *Large Igneous Provinces: Continental, Oceanic and Planetary Flood Volcanism, Am. Geophys. Union Geophys. Monog.*, vol. 100. American Geophysical Union, Washington, DC, pp. 183–216.

Neal, C.R., Taylor, L.A., Davidson, J.P., Holden, P., Halliday, A.N., Nixon, P.H., Paces, J.B., Clayton, R.N., Mayeda, T.K., 1990. Eclogites with oceanic and mantle signatures from the Bellsbank kimberlite, South Africa, part 2: Sr, Nd, and O isotope geochemistry. *Earth Planet. Sci. Lett.* **99**, 362–379.

Nichols, G.T., Wyllie, P.J., Stern, C.R., 1994. Subduction zone melting of pelagic sediments constrained by melting experiments. *Nature* **371**, 785–788.

Nielsen, S.G., Baker, J.A., Krogstad, E.J., 2002. Petrogenesis of an early Archaean (3.4 Ga) norite dyke, Isua, West Greenland: evidence for early Archaean crustal recycling? *Prec. Res.* **118**, 133–148.

Nisbet, E.G., Cheadle, M.J., Arndt, N.T., Bickle, M.J., 1993. Constraining the potential temperature of the Archaean mantle—a review of the evidence from komatiites. *Lithos* **30**, 291–307.

Niu, F.L., James, D.E., 2002. Fine structure of the lowermost crust beneath the Kaapvaal craton and its implications for crustal formation and evolution. *Earth Planet. Sci. Lett.* **200**, 121–130.

Niu, Y.L., 1997. Mantle melting and melt extraction processes beneath ocean ridges: evidence from abyssal peridotites. *J. Petrol.* **38**, 1047–1074.

Parman, S.W., Grove, T.L., 2004. Harzburgite melting with and without H_2O: experimental data and predictive modeling. *J. Geophys. Res.* **109**. doi:10.1029/2003JB002566, art. B02201.

Parman, S.W., Grove, T.L., Dann, J.C., 2001. The production of Barberton komatiites in an Archean subduction zone. *Geophys. Res. Lett.* **28**, 2513–2516.

Parman, S.W., Grove, T.L., Dann, J.C., de Wit, M.J., 2004. A subduction origin for komatiites and cratonic lithospheric mantle. *S. Afr. J. Geol.* **107**, 107–118.

Patino, L.C., Carr, M.J., Feigenson, M.D., 2000. Local and regional variations in Central American arc lavas controlled by variations in subducted sediment input. *Contrib. Mineral. Petr.* **138**, 265–283.

Patiño-Douce, A.E., Johnston, A.D., 1991. Phase equilibria and melt productivity in the pelitic system—implications for the origin of peraluminous granitoids and aluminous granulites. *Contrib. Mineral. Petr.* **107**, 202–218.

Peacock, S.M., Rushmer, T., Thompson, A.B., 1994. Partial melting of subducting oceanic crust. *Earth Planet. Sci. Lett.* **121**, 227–244.

Pearce, J.A., 1982. Trace element characteristics of lavas from destructive plate boundaries. In: Thorpe, R.S. (Ed.), *Andesites*. Wiley, New York, pp. 525–548.

Pearson, D.G., 1999. The age of continental roots. *Lithos* **48**, 171–194.

Pearson, D.G., Carlson, R.W., Shirey, S.B., Boyd, F.R., Nixon, P.H., 1995. Stabilisation of Archaean lithospheric mantle: a Re-Os isotope study of peridotite xenoliths from the kaapvaal craton. *Earth Planet. Sci. Lett.* **134**, 341–357.

Peck, W.H., Valley, J.W., Wilde, S.A., Graham, C.M., 2001. Oxygen isotope ratios and rare earth elements in 3.3 to 4.4 Ga zircons: ion microprobe evidence for high delta O-18 continental crust and oceans in the Early Archean. *Geochim. Cosmochim. Acta* **65**, 4215–4229.

Percival, J.A., McNicoll, V., Brown, J.L., Whalen, J.B., 2004. Convergent margin tectonics, central Wabigoon subprovince, Superior Province, Canada. *Prec. Res.* **132**, 213–244.

Percival, J.A., Mortensen, J.K., 2002. Water-deficient calc-alkaline plutonic rocks of northeastern Superior Province, Canada: Significance of charnockitic magmatism. *J. Petrol.* **43**, 1617–1650.

Percival, J.A., Skulski, T., 2000. Tectonothermal evolution of the northern Minto block, Superior Province, Quebec, Canada. *Can. Mineral.* **38**, 345–378.

Perugini, D., Busa, T., Poli, G., Nazzareni, S., 2003. The role of chaotic dynamics and flow fields in the development of disequilibrium textures in volcanic rocks. *J. Petrol.* **44**, 733–756.

Petford, N., Gallagher, K., 2001. Partial melting of mafic (Amphibolitic) lower crust by periodic influx of basaltic magma. *Earth Planet. Sci. Lett.* **193**, 483–499.

Pickering-Witter, J., Johnston, A.D., 2000. The effects of variable bulk composition on the melting systematics of fertile peridotitic assemblages. *Contrib. Mineral. Petrol.* **140**, 190–211.

Piper, J.D.A., 2003. Consolidation of continental crust in late Archaean-early Proterozoic times: a palaeomagnetic test. *Gondwana Res.* **6**, 435–448.

Pollack, H.N., 1997. Thermal characteristics of the Archa ean. In: de Wit, M.J., Ashwal, L.D. (Eds.), *Greenstone Belts*. Oxford Science Publications, Oxford, pp. 223–232.

Poudjom Djomani, Y.H., O'Reilly, S.Y., Griffin, W.L., Morgan, P., 2001. The density structure of subcontinental lithosphere through time. *Earth Planet. Sci. Lett.* **184**, 605–621.

Presnall, D.C., Dixon, J.R., O'Donnell, T.H., Dixon, S.A., 1979. Generation of mid-ocean ridge tholeiites. *J. Petrol.* **20**, 3–35.

Prokoph, A., Ernst, R.E., Buchan, K.L., 2004. Time-series analysis of large igneous provinces: 3500 Ma to present. *J. Geol.* **112**, 1–22.

Prowatke, S., Klemme, S., 2005. Effect of melt composition on the partitioning of trace elements between titanite and silicate melt. *Geochim. Cosmochim. Acta* **69**, 695–709.

Rai, S.S., Priestley, K., Suryaprakasam, K., Srinagesh, D., Gaur, V.K., Du, Z., 2003. Crustal shear velocity of the south Indian shield. *J. Geophys. Res.* **108**. doi:10.1029/2002JB001776, art. 2088.

Rapp, R.P., Shimizu, N., Norman, M.D., 2003. Growth of early continental crust by partial melting of eclogite. *Nature* **425**, 605–609.

Rapp, R.P., Watson, E.B., 1995. Dehydration melting of metabasalt at 8–32 kbar: implications for continental growth and crust-mantle recycling. *J. Petrol.* **36**, 891–931.

Rapp, R.P., Watson, E.B., Miller, C.F., 1991. Partial melting of amphibolite eclogite and the origin of Archean trondhjemites and tonalites. *Prec. Res.* **51**, 1–25.

Révillon, S., Chauvel, C., Arndt, N.T., Pik, R., Martineau, F., Fourcade, S., Marty, B., 2002. Heterogeneity of the Caribbean plateau mantle source: Sr, O and He isotopic compositions of olivine and clinopyroxene from Gorgona Island. *Earth Planet. Sci. Lett.* **205**, 91–106.

Rey, P.F., Philippot, P., Thébaud, N., 2003. Contribution of mantle plumes, crustal thickening and greenstone blanketing to the 2.75-2.65 Ga global crisis. *Prec. Res.* **127**, 43–60.

Richardson, S.H., Gurney, J.J., Erlank, A.K., Harris, J.W., 1984. Origin of diamonds in old enriched mantle. *Nature* **310**, 198–202.

Richter, F.M., 1985. Models for the Archean thermal regime. *Earth Planet. Sci. Lett.* **73**, 350–360.

Ridley, J.R., 1992. On the origins and tectonic significance of the charnockite suite of the Archaean Limpopo Belt, Northern Marginal Zone, Zimbabwe. *Prec. Res.* **55**, 407–427.

Ridley, J.R., Vearncombe, J.R., Jelsma, H.A., 1997. Relations between greenstone belts and associated granitoids. In: de Wit, M.J., Ashwal, L.D. (Eds.), *Greenstone Belts*. Oxford Science Publications, Oxford, pp. 376–397.

Rollinson, H., 1997. Eclogite xenoliths in west African kimberlites as residues from Archaean granitoid crust formation. *Nature* **389**, 173–176.

Rollinson, H.R., Tarney, J., 2005. Adakites—the key to understanding LILE depletion in granulites. *Lithos* **79**, 61–81.

Rollinson, H.R., Windley, B.F., 1980. An Archaean granulite–grade, tonalite-trondhjemite-granite suite from Scourie, NW Scotalnd: Geochemistry and origin. *Contrib. Mineral. Petr.* **72**, 265–281.

Rudnick, R.L., 1995. Making continental crust. *Nature* **378**, 571–578.

Rudnick, R.L., Barth, M., Horn, I., McDonough, W.F., 2000. Rutile-bearing refractory eclogites: missing link between continents and depleted mantle. *Science* **287**, 278–281.

Rudnick, R.L., Taylor, S.R., 1986. Geochemical constraints on the origin of Archaean tonalitic—trondhjemitic rocks and implications for lower crustal composition. In: Dawson, J.B., Carswell, D.A., Hall, J., Wedepohl, K.H. (Eds.), *The Nature of the Lower Continental Crust*, vol. 24. Geol. Soc. Lond. Spec. Publ., Geol. Soc. London Publishing House, Brassmill Enterprises, Bath, UK, pp. 179–191.

Rushmer, T., 1991. Partial melting of two amphibolites: contrasting experimental results under fluid-absent conditions. *Contrib. Mineral. Petr.* **107**, 41–59.

Ryerson, F.J., Watson, E.B., 1987. Rutile saturation in magmas: implications for Ti–Nb–Ta depletion in island-arc basalts. *Earth Planet. Sci. Lett.* **86**, 225–239.

Saleeby, J., Ducea, M., Clemens-Knott, D., 2003. Production and loss of high-density batholithic root, southern Sierra Nevada, California. *Tectonics* **22**. doi:10.1029/2002TC001374, art. 1064.

Sandiford, M., 1989. Horizontal structures in granulite terrains: a record of mountain building or mountain collapse? *Geology* **17**, 449–452.

Sandiford, M., Van Kranendonk, M., Bodorkos, S., 2004. Conductive incubation and the origin of granite-greenstone dome and keel structure: the Eastern Pilbara Craton, Australia. *Tectonics* **23**. doi:10.1029/2002TC001452, art. C1009.

Saunders, A.D., Tarney, J., Kerr, A.C., Kent, R.W., 1996. The formation and fate of large oceanic igneous provinces. *Lithos* **37**, 81–95.

Schafer, S.J., Morton, P., 1991. Two komatiitic pyroclastic units, Superior Province, northwestern Ontario: their geology, petrography and correlation. *Can. J. Earth Sci.* **28**, 1455–1470.

Schiano, P., Clocchiatti, R., Shimizu, N., Maury, R.C., Jochum, K.P., Hofmann, A.W., 1995. Hydrous, silica-rich melts in the sub-arc mantle and their relationship with erupted arc lavas. *Nature* **377**, 595–600.

Schmidberger, S.S., Simonetti, A., Francis, D., Gariépy, C., 2002. Probing Archean lithosphere using the Lu-Hf isotopic systematics of peridotite xenoliths from Sometrset Island kimberlites, Canada. *Earth Planet. Sci. Lett.* **197**, 245–259.

Schmidt, M.W., Thompson, A.B., 1996. Epidote in calc-alkaline magmas: an experimental study of stability, phase relationships, and the role of epidote in magmatic evolution. *Am. Mineral.* **81**, 462–474.

Schulze, D.J., Valley, J.W., Spicuzza, M.J., 2000. Coesite eclogites from the Roberts Victor Kimberlite, South Africa. *Lithos* **54**, 23–32.

Shaw, H.R., Jackson, E.D., 1973. Linear island chains in the Pacific: result of thermal plumes of gravitational anchors? *J. Geophys. Res.* **78**, 8634–8652.

Shirey, S.B., Carlson, R.W., Richardson, S.H., Menzies, A., Gurney, J.J., Pearson, D.G., Harris, J.W., Wiechert, U., 2001. Archean emplacement of eclogitic components into the lithospheric mantle during formation of the Kaapvaal Craton. *Geophys. Res. Lett.* **28**, 2509–2512.

Shirey, S.B., Hanson, G.N., 1986. Mantle heterogeneity and crustal recycling in Archean granite-greenstone belts: evidence from Nd isotopes and trace elements in the Rainy Lake area, Superior Province, Ontario, Canada. *Geochim. Cosmochim. Acta* **50**, 2631–2651.

Simon, N.S.C., Irvine, G.J., Davies, G.R., Pearson, D.G., Carlson, R.W., 2003. The origin of garnet and clinopyroxene in "depleted" Kaapvaal peridotites. *Lithos* **71**, 289–322.

Sleep, N.H., Windley, B.F., 1982. Archean plate tectonics: constraints and inferences. *J. Geol.* **90**, 363–379.

Smithies, R.H., 2000. The Archaean tonalite-trondhjemite-granodiorite (TTG) series is not an analogue of Cenozoic adakite. *Earth Planet. Sci. Lett.* **182**, 115–125.

Smithies, R.H., 2002. Archaean boninite-like rocks in an intracratonic setting. *Earth Planet. Sci. Lett.* **197**, 19–34.

Smithies, R.H., Champion, D.C., Cassidy, K.F., 2003. Formation of earth's early Archaean continental crust. *Prec. Res.* **127**, 89–101.

Snyder, G.A., Taylor, L.A., Crozaz, G., Halliday, A.N., Beard, B.L., Sobolev, V.N., Sobolev, N.V., 1997. The origins of Yakutian eclogite xenoliths. *J. Petrol.* **38**, 85–113.

Sproule, R.A., Lesher, C.M., Ayer, J.A., Thurston, P.C., Herzberg, C.T., 2002. Spatial and temporal variations in the geochemistry of komatiites and komatiitic basalts in the Abitibi greenstone belt. *Prec. Res.* **115**, 153–186.

Stern, R.A., Hanson, G.N., 1991. Archean high-Mg granodiorite: a derivative of light rare earth element-enriched monzodiorite of mantle origin. *J. Petrol.* **32**, 201–238.

Stern, R.A., Percival, J.A., Mortensen, J.K., 1994. Geochemical evolution of the minto block: a 2.7 Ga continental magmatic arc built on the Superior proto-craton. *Prec. Res.* **65**, 115–153.

Stern, R.J., 2005. Evidence from ophiolites, blueschists, and ultrahigh-pressure metamorphic terranes that the modern episode of subduction tectonics began in Neoproterozoic time. *Geology* **33**, 557–560.

Stevenson, R., Henry, P., Gariépy, C., 1999. Assimilation-fractional crystallization origin of Archean Sanukitoid Suites: Western Superior Province, Canada. *Prec. Res.* **96**, 83–99.

Strik, G., Blake, T.S., Zegers, T.E., White, S.H., Langereis, C.G., 2003. Palaeomagnetism of flood basalts in the Pilbara Craton, Western Australia: Late Archaean continental drift and the oldest known reversal of the geomagnetic field. *J. Geophys. Res.* **108**. doi:10.1029/2003JB002475, art. 2551.

Sun, S.-S., McDonough, W.F., 1989. Chemical and isotopic systematics of oceanic basalts: implications for mantle compositions and processes. In: Saunders, A.D., Norry, M.J. (Eds.), *Magmatism in the Ocean Basins*, vol. 42. Geol. Soc. London Spec. Publ., Geol. Soc. London Publishing House, Brassmill Enterprises, Bath, UK, pp. 313–345.

Sutcliffe, R.H., Smith, A.R., Doherty, W., Barnett, R.L., 1990. Mantle derivation of Archean amphibole-bearing granitoid and associated mafic rocks: Evidence from the southern Superior Province, Canada. *Contrib. Mineral. Petr.* **105**, 255–274.

Sylvester, P.J., Campbell, I.H., Bowyer, D.A., 1997. Niobium/uranium evidence for early formation of the continental crust. *Science* **275**, 521–523.

Takahashi, E., Nakajima, K., Wright, T.L., 1998. Origin of the Columbia River basalts: melting model of a heterogeneous plume head. *Earth Planet. Sci. Lett.* **162**, 63–80.

Tarney, J., Dalziel, W.D., de Wit, M.J., 1976. Marginal basin ''Rocas Verdes'' complex from S. Chilea model for Archean greenstone belt formation. In: Windley, B.F. (Ed.), *The Early History of the Earth*. Wiley-Interscience, London, pp. 131–146.

Tarney, J., Weaver, B., Drury, S.A., 1979. Geochemistry of Archaean trondhjemitic and tonalitic gneisses from Scotland and East Greenland. In: Barker, F. (Ed.), *Trondhjemites, Dacites, and Related Rocks*. Elsevier, Amsterdam, pp. 275–299.

Tatsumi, Y., 2000. Continental crust formation by crustal delamination in subduction zones and complementary accumulation of the enriched mantle I component in the mantle. *Geochem. Geophys. Geosyst.* **1**. doi:10.1029/2000GC000094.

Taylor, S.R., McLennan, S.M., 1986. The geochemical composition of the Archaean ctrust. In: Dawson, J.B., Carswell, D.A., Hall, J., Wedepohl, K.H. (Eds.), *The Nature of the Lower Continental Crust*, vol. 24. Geol. Soc. London Spec. Publ., Geol. Soc. London Publishing House, Brassmill Enterprises, Bath, UK, pp. 173–178.

Tejada, M.L.G., Mahoney, J.J., Duncan, R.A., Hawkins, M.P., 1996. Age and geochemistry of basement and alkalic rocks of Malaita and Santa Isabel, Solomon islands, southern margin of Ontong Java Plateau. *J. Petrol.* **37**, 361–394.

Tejada, M.L.G., Mahoney, J.J., Neal, C.R., Duncan, R.A., Petterson, M.G., 2002. Basement geochemistry and geochronology of central Malaita, Solomon islands, with implications for the origin and evolution of the Ontong Java Plateau. *J. Petrol.* **43**, 449–484.

Thurston, P.C., 1994. Archean volcanic patterns. In: Condie, K.C. (Ed.), *Archean Crustal Evolution*, *Developments in Precambrian Geology*, vol. 11. Elsevier, Amsterdam, pp. 45–84.

Thurston, P.C., 2002. Autochthonous development of Superior Province greenstone belts? *Prec. Res.* **115**, 11–36.

Tiepolo, M., Oberti, R., Vannucci, R., 2002. Trace-element incorporation in titanite: constraints from experimentally determined solid/liquid partition coefficients. *Chem. Geol.* **191**, 105–119.

Tomlinson, K.Y., Davis, D.W., Stone, D., Hart, T.R., 2003. U-Pb age and Nd isotopic evidence for Archean terrane development and crustal recycling in the south-central Wabigoon subprovince, Canada. *Contrib. Mineral. Petr.* **144**, 684–702.

Tomlinson, K.Y., Hughes, D.J., Thurston, P.C., Hall, R.P., 1999. Plume magmatism and crustal growth at 2.9 to 3.0 Ga in the Steep Rock and Lumby Lake area, Western Superior Province. *Lithos* **46**, 103–136.

Tomlinson, K.Y., Stott, G.M., Percival, J.A., Stone, D., 2004. Basement terrane correlations and crustal recycling in the western Superior Province: Nd isotopic character of granitoid and felsic volcanic rocks in the Wabigoon subprovince, N.Ontario, Canada. *Prec. Res.* **132**, 245–274.

Van Hunen, J., van den Berg, A.P., Vlaar, N.J., 2004. Various mechanisms to induce present-day shallow flat subduction and implications for the younger Earth: a numerical parameter study. *Phys. Earth Planet. Int.* **146**, 179–194.

van Keken, P.E., Kiefer, B., Peacock, S.M., 2002. High-resolution models of subduction zones: Implications for mineral dehydration reactions and the transport of water into the deep mantle. *Geochem. Geophys. Geosyst.* **3**. doi:10.1029/2001GC000256, art. 1056.

Van Kranendonk, M.J., Collins, W.J., Hickman, A., Pawley, M.J., 2004. Critical tests of vertical vs. horizontal tectonic models for the Archaean East Pilbara Granite-Greenstone Terrane, Pilbara Craton, Western Australia. *Prec. Res.* **131**, 173–211.

Van Kranendonk, M.J., Hickman, A.H., Smithies, R.H., Nelson, D.R., Pike, G., 2002. Geology and tectonic evolution of the archean North Pilbara terrain, Pilbara Craton, Western Australia. *Econ. Geol.* **97**, 695–732.

van Thienen, P., van den Berg, A.P., Vlaar, N.J., 2004a. On the formation of continental silicic melts in thermochemical mantle convection models: implications for early Earth. *Tectonophysics* **394**, 111–124.

van Thienen, P., van den Berg, A.P., Vlaar, N.J., 2004b. Production and recycling of oceanic crust in the early Earth. *Tectonophysics* **386**, 41–65.

Vervoort, J.D., Patchett, P.J., 1996. Behavior of hafnium and neodymium isotopes in the crust: Constraints from Precambrian crustally derived granites. *Geochim. Cosmochim. Acta* **60**, 3717–3733.

Vlaar, N.J., van Keken, P.E., van den Berg, A.P., 1994. Cooling of the Earth in the Archaean: consequences of pressure-release melting in a hotter mantle. *Earth Planet.Sci. Lett.* **121**, 1–18.

Walter, M.J., 1998. Melting of garnet peridotite and the origin of komatiite and depleted lithosphere. *J. Petrol.* **39**, 29–60.

Wang, P., Glover, L.I., 1992. A tectonics test of the most commonly used geochemical discriminant diagrams and patterns. *Earth Sci. Rev.* **33**, 111–131.

Wasylenki, L.E., Baker, M.B., Kent, A.J.R., Stolper, E.M., 2003. Near-solidus melting of the shallow upper mantle: partial melting experiments on depleted peridotite. *J. Petrol.* **44**, 1163–1191.

Weaver, B.L., Tarney, J., 1980. Rare-earth geochemistry of Lewisian granulite-facies gneisses, northwest Scotland: implications for the petrogenesis of the Archean lower continental crust. *Earth Planet. Sci. Lett.* **51**, 279–296.

Weaver, B.L., Tarney, J., 1981. Lewisian gneiss geochemistry and Archaean crustal development models. *Earth Planet. Sci. Lett.* **55**, 171–180.

Wedepohl, K.H., 1995. The composition of the continental crust. *Geochim. Cosmochim. Acta* **59**, 1217–1232.

Whalen, J.B., McNicoll, V.J., Galley, A.G., Longstaffe, F.J., 2004a. Tectonic and metallogenic importance of an Archean composite high- and low-Al tonalite suite, Western Superior Province, Canada. *Prec. Res.* **132**, 275–301.

Whalen, J.B., Percival, J.A., McNicoll, V.J., Longstaffe, F.J., 2004b. Geochemical and isotopic (Nd-O) evidence bearing on the origin of late- to post-orogenic high-K granitoid rocks in the Western Superior Province: implications for Late Archean tectonomagmatic processes. *Prec. Res.* **132**, 303–326.

Whalen, J.B., Percival, J.A., McNicoll, V.J., Longstaffe, F.J., 2002. A mainly crustal origin for tonalitic granitoid rocks, Superior Province, Canada: Implications for Late Archean tectonomagmatic processes. *J. Petrol.* **43**, 1551–1570.

Whitehouse, M.J., Kalsbeek, F., Nutman, A.P., 1998. Crustal growth and crustal recycling in the Nagssugtoqidian orogen of West Greenland: Constraints from radiogenic isotope systematics and U-Pb zircon geochronology. *Prec. Res.* **91**, 365–381.

Williams, H., 1990. Subprovince accretion tectonics in the south-central Superior Province. *Can. J. Earth Sci.* **27**, 570–581.

Windley, B.F., 1984. In: *The Evolving Continents*. Wiley, London, NY, p. 399.

Windley, B.F., Davies, F.B., 1978. Volcano spacings and lithospheric/crustal thickness in the Archaean. *Earth Planet. Sci. Lett.* **38**, 291–297.

Winter, J.D., 2001. *An Introduction to Igneous and Metamorphic Petrology*. Prentice-Hall, New York, p. 699.

Workman, R.K., Hart, S.R., 2005. Major and trace element composition of the depleted MORB mantle (DMM). *Earth Planet. Sci. Lett.* **231**, 53–72.

Wyllie, P.J., Huang, W., Stern, C.R., Maaloe, S., 1976. Granitic magmas: possible and impossible sources, water contents, and crystallization sequences. *Can. J. Earth Sci.* **13**, 1007–1019.

Wyman, D.A., Kerrich, R., 2002. Formation of Archean continental lithospheric roots: the role of mantle plumes. *Geology* **30**, 543–546.

Wyman, D.A., Kerrich, R., Polat, A., 2002. Assembly of Archean cratonic mantle lithosphere and crust: plume-arc interaction in the Abitibi-Wawa subduction-accretion complex. *Prec. Res.* **115**, 37–62.

Yasuda, A., Fujii, T., 1998. Ascending subducted oceanic crust entrained within mantle plumes. *Geophys. Res. Lett.* **25**, 1561–1564.

Yasuda, A., Fujii, T., Kurita, K., 1997. A composite diapir model for extensive basaltic volcanism: magmas from subducted oceanic crust entrained within mantle plumes. *Proc. Jpn. Acad. Sci.* **73B**, 201–204.

Yaxley, G.M., 2000. Experimental study of the phase and melting relations of homogeneous basalt plus peridotite mixtures and implications for the petrogenesis of flood basalts. *Contrib. Mineral. Petr.* **139**, 326–338.

Yaxley, G.M., Green, D.H., 1998. Reactions between eclogite and peridotite: Mantle refertilisation by subduction of oceanic crust. *Schweiz. Mineral. Petrogr. Mitt.* **78**, 243–255.

Zack, T., Tomascak, P.B., Rudnick, R.L., Dalpé, C., McDonough, W.F., 2003. Extremely light Li in orogenic eclogites: the role of isotope fractionation during dehydration in subducted oceanic crust. *Earth Planet. Sci. Lett.* **208**, 279–290.

Zegers, T.E., van Keken, P.E., 2001. Middle Archean continent formation by crustal delamination. *Geology* **29**, 1083–1086.

Zhai, M.G., Zhao, G.C., Zhang, Q., 2002. Is the Dongwanzi complex an Archean ophiolite? *Science* **295**, U1.

Zheng, J.P., O'Reilly, S.Y., Griffin, W.L., Lu, F.X., Zhang, M., Pearson, N.J., 2001. Relict refractory mantle beneath the eastern North China block: significance for lithosphere evolution. *Lithos* **57**, 43–66.